First Principles Study of Ternary Skutterudites

by

An Li

B.S., Electrical Engineering and Computer Science
Massachusetts Institute of Technology (2010)

Submitted to the Department of Electrical Engineering and Computer Science
in Partial Fulfillment of the Requirements for the Degree of
Master of Engineering in Electrical Engineering and Computer Science
at the Massachusetts Institute of Technology

September 2011

Author .....
Department of Electrical Engineering and Computer Science
September, 2011

Certified by .....
Gang Chen
Carl Richard Soderberg Professor of Power Engineering
Thesis Supervisor

Certified by .....
Boris Kozinsky
Sr. Research Scientist at Robert Bosch Research and Technology Center
Thesis Co-Supervisor

Accepted by .....
Prof. Dennis M. Freeman
Chairman, Masters of Engineering Thesis Committee

First Principles Study of Ternary Skutterudites

by

An Li

Submitted to the Department of Electrical Engineering and Computer Science

September 2011
in Partial Fulfillment of the Requirements for the Degree of Master of Engineering
in Electrical Engineering and Computer Science

Abstract

As the demand of sustainable energy technologies increases in recent years, thermoelectric materials can potentially become a solution by increasing energy efficiency in certain systems, such as waste heat recovery system. Skutterudites is a popular group of thermoelectric materials because they show low thermal conductivity with filled voids in their structures.

To investigate the potential of ternary skutterudites as thermoelectric materials, first-principles calculations are performed on filled and unfilled $CoSn_{1.5}S_{1.5}$, $CoSn_{1.5}Se_{1.5}$, $CoSn_{1.5}Te_{1.5}$, $CoGe_{1.5}S_{1.5}$, $CoGe_{1.5}Se_{1.5}$, and $CoGe_{1.5}Te_{1.5}$. Alkaline-earth metal and Lanthanum are used as void fillers in this study. Transport properties, including Seebeck coefficient and electrical conductivity, are obtained from Boltzmann transport theory. The calculation results show high Seebeck coefficients and low electrical conductivities. Future work will focus on increasing the electrical conductivity while reducing the thermal conductivity with appropriate filling.

Thesis Supervisor: Gang Chen
Title: Carl Richard Soderberg Professor of Power Engineering

Acknowledgements

First of all, I would like to thank Dr. Boris Kozinsky and Dr. Roel Sanchez-Carrera, with whom I worked and learned from for half a year. Their technical expertise has been invaluable in allowing me to learn the field and start my research.

Second, I would like to thank Professor Gang Chen for taking me as his advisee and providing me his guidance on my research and thesis. I would further like to thank Dr. Daehyun Wee, Professor Marco Fornari, and Dmitri Volja for their discussions and advices.

Lastly, I should thank my family and friends for their love and support.

Table of Contents

Chapter 1: Introduction

1.1 Motivation

Energy shortage and environment problem has become a worldwide issue in the last few decades. The use of oil, coal and other fossil energy sources is polluting the planet with greenhouse gases. The united States produces about 2 billion tons of CO2 annually from coal-burning power plants [1]. The vast majority of the world's power is generated with low efficiency. Thus, roughly 15 terawatts of power is lost to the environment in the form of waste heat [2]. As people are trying different methods to solve this crisis, thermoelectric devices have been a potential solution for many years [3]. The unique feature of thermoelectric material is that it can convert energy between heat and electricity directly. Devices based on the thermoelectric effect could be used to convert this waste heat into useful electricity and to pump heat. There are two primary areas in which thermoelectric devices can lend themselves to increase energy efficiency and decrease pollutants: electricity generation and refrigeration.

Power-generation applications are currently being investigated by the automotive industry as a means to generate electrical power from waste engine heat from the radiator and the exhaust systems for use in next-generation vehicles. In traditional vehicles, internal combustion engines are highly inefficient in energy.

Only 20- 25% of the energy generated during fuel combustion is used [4]. Furthermore, the electricity requirement in vehicles is increasing due to the demands of enhanced performance, on-board controls and stability controls, navigation systems, etc. In order to gain fuel efficiency, it may be possible to draw energy from the engine to the electrical load in the car. Thermoelectric devices are thus being investigated to convert waste heat into usable electricity energy. An example of thermoelectric generator is the radioisotope thermoelectric generators for NASA's deep space missions that have been developed and in use since 1970s [5].

Thermoelectric refrigeration is a green method for small-scale, localized cooling. There is a great need for such cooling method in computers, electronics, and optoelectronics as well as many other applications. If significant economical cooling can be achieved, the resulting cold computing could produce speed gain of 30%-200% in some computer processors based on CMOS technology [6]. Thermoelectric refrigeration is also used in the synthesis of DNA by polymerase chain reaction and on spacecrafts to counter the effect of direct sunlight on one side of a craft [7].

However, current thermoelectric devices are too inefficient to be cost effective in most applications. They have low efficiency because of the lack of good thermoelectric materials. Current devices are only used for niche applications where efficiency is outweighed by the need for reliability, lightweight, and small

size, such as NASA space missions [5]. Thus, the demand for high efficiency thermoelectric materials is very high.

1.2 Thermoelectric Material

Thermoelectric (TE) materials are materials that show strong thermoelectric effects. Cost effective thermoelectric materials could be used in devices for power generation and refrigeration. In addition to TE performance, viable TE materials should also have the following properties: high mechanical strength, high thermal shock resistance, ease of manufacturing, low cost and toxicity, and thermal expansion compatibility with other device components.

1.2.1 Seebeck Effect and Peltier Effect

Seebeck effect is one of the most fundamental thermoelectric phenomena. In early 1800s, Thomas Seebeck observed that when two dissimilar materials are joined together and their junctions are maintained at two different temperatures, a voltage difference proportional to the temperature difference is produced [8]. The ratio of the voltage gradient developed to the temperature gradient is related to an intrinsic property of the materials called the Seebeck coefficient $S=-dV/dT$. The sign of the coefficient is negative when the generated electric field has the same direction of the thermal current. In semi-conducting material, S is positive for p-type material and negative for n-type material.

Another fundamental thermoelectric phenomena, the Peltier effect, was discovered by Jean Peltier, who found that when an electrical current is applied through the junction of two dissimilar metals, heat is either absorbed or rejected at the junction, depending on the direction of the current [8]. Peltier effect and Seebeck effect have been later shown to be related to each other. The definition of the Peltier coefficient, Π=S*T. The rate at which the Peltier heat is liberated or rejected at the junction is given by Q=Π*I, where I is the current through the junction.

1.2.2 Figure of Merit

A material's figure of merit, ZT, is a good measurement of its potential for thermoelectric applications [9] as it is related to the overall heat-to-electricity conversion efficiency in a device. Z is defined as

$$Z = \frac{\sigma S^2}{\kappa} \qquad (1.1)$$

where S is the Seebeck coefficient, σ is the electrical conductivity, and κ is the total thermal conductivity ($\kappa = \kappa\_l + \kappa\_e$, the lattice and electronic contributions, respectively). The dimensionless figure of merit ZT is Z multiplied with temperature T. The efficiency of ideal thermoelectric devices can be expressed as

$$\eta = \frac{T_h - T_c}{T_h} \frac{\sqrt{1+(ZT)_M} - 1}{\sqrt{1+(ZT)_M} + \frac{T_c}{T_h}} \qquad (1.2)$$

where T_c is the cold-side temperature, T_h is the hot-side temperature, and (ZT)M is the effective ZT of the thermoelectric material between T_c and T_h [9].

The best TE materials currently used in most commercial devices have ZT = 1 [10]. This value has been a practical upper limit for several decades, yet there are no theoretical or thermodynamic reasons for ZT= 1 as an upper barrier [10]. As seen from equation (1.1), ZT can be increased by decreasing κ_l or by increasing σ or S. However, σ is tied to the electronic thermal conductivity, κ_e, through the Wiedemann–Franz law, which states that the ratio of the electronic contribution to the thermal conductivity and the electrical conductivity of a metal is proportional to the temperature [11].

1.2.3 Thermoelectric Devices

The basic structure of a thermoelectric module is illustrated in figure 1.1, which shows a thermoelectric couple composed of a n-type and a p-type semiconductor material connected through metallic electrical contact pads. Both refrigeration and power generation may be accomplished using the same module. Thermoelectric devices are usually built up of an array of these couples, arranged electrically in series and thermally in parallel [12].

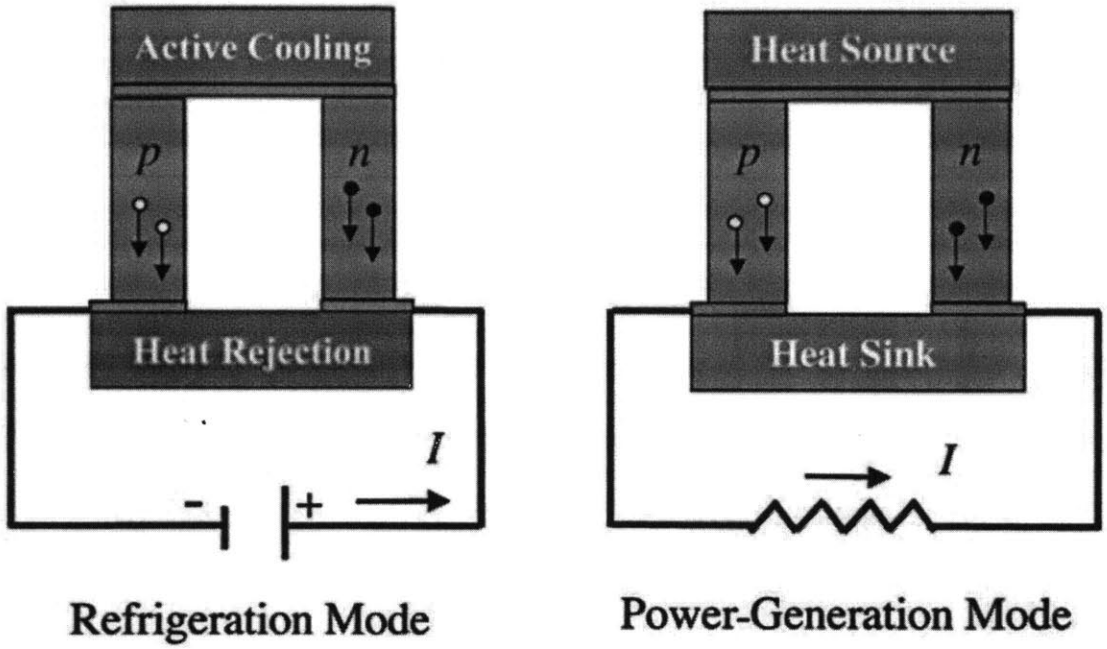

Figure 1.1 Diagram of a thermoelectric couple made of n-type and p-type thermoelectric materials [12].

Thermoelectric energy conversion utilizes the Seebeck effect, wherein a temperature gradient is imposed across the device, resulting in a voltage that can be used to drive a current through a load device. This is the direct conversion of heat into electricity.

Conversely, the Peltier heat is generated when an electric current is passed through a junction made of two TE materials. The head is extracted at one side and rejected at the other side thus creating a temperature gradient. The

advantages of TE solid-state energy conversion are compactness, quietness, and localized heating or cooling.

1.3 Objectives and Outline

Currently, there is no convincing theory on the thermodynamic limits to the possible values of ZT. Proposed applications of thermoelectric materials are demanding higher performance thermoelectric materials than those that are currently in use. The usage of computer simulation in estimating material properties can make the discovery process automatic and fast.

In recent years, the $CoSb_3$ based skutterudite thermoelectric materials have attracted much attention due to the feature of voids in their structures. Filling the voids can reduce its thermal conductivity but maintain its excellent electrical properties. Ternary skutterudites are isoelectronic to binary skutterudites, thus they may have similar good transport properties.

The goal for this study is to investigate the potential of ternary skutterudites as thermoelectric materials using ab initio calculations. We would like to know the theoretical values of their transport properties such as the Seebeck coefficients and electrical conductivities. Chapter One introduces the basic background of thermoelectric materials. Chapter Two explains the ab initio calculation methods as well as the calculation tools we use in our study. Chapter Three shows the

detailed results of our calculation for both filled and unfilled ternary skutterudites, including crystal structure, density of states, and transport properties. Chapter Four discusses the potential of ternary skutterudites as thermoelectric materials by analyzing the calculation results. A simple method for determining the stability of a compound is also introduced in chapter four. The last chapter, chapter five, talks about the future research direction on ternary skutterudites.

Chapter 2: Methodology

2.1 Ab Initio Calculations

Ab initio calculations are used to predict the physical properties of materials without using any experimental inputs. All physical characteristics should be determined on the sole knowledge of the constituent atoms without uncontrolled simplifications. The atomic structure must be first obtained, from which all electronic, magnetic and vibration properties could be extracted.

Density functional theory provides the theoretical background for such studies by demonstrating how features of many-electron systems encountered in atoms, molecules, and solids, can be determined by using a single-electron functional, which in this case is the electronic density [13]. Even in the simplest cases, to obtain the electronic density from first-principles is a task that cannot be accomplished analytically and requires large-scale calculations on dedicated computers.

Nowadays, with the continuous increase in available computational power and refined theoretical techniques, ab initio computation has become a powerful tool for researchers to search for new materials and understand experimental results.

2.2 Density Functional Theory

In brief, density-functional theory (DFT) attempts to solve the many-body problems by recasting the time-independent Schrodinger equation as a functional of one variable, the charge density n(r).

The starting point is the stationary Schrodinger equation for a N-electron system in a given external potential $v_{ext}(r)$, which we seek to solve :

$$\left[-\frac{h^2}{2m}\sum_{i=1}^{N}\nabla_i^2+\sum_{i=1}^{N}v_{ext}(r_i)+\tfrac{1}{2}\sum_{i\neq j}\frac{e^2}{|r_i-r_j|}\right]\Psi(r_1,\ldots,r_N)=E\Psi(r_1,\ldots,r_N) \qquad (2.1)$$

The first term in equation (2.1) gives the electronic kinetic energy, the second gives the effect of the external potential and the third gives the electron-electron interaction [13]. The huge number of particles obviously makes the direct resolution of this equation impossible. Fortunately, from an experimental point of view, we are not interested in the full many-body wave function, but only in contracted quantities such as the electronic density and total energy.

A rigorous theorem by Hohenberg and Kohn [14], which is the basis of DFT , shows that the knowledge of the ground-state electronic density n(r) is sufficient to determine all the physical properties of the system. In particular, the ground state electronic density is proven to determine the external potential $v_{ext}(r)$ as well

as the total number of particles N. The full Hamiltonian and all properties derived from it are thus uniquely determined by n(r). Furthermore, a variational principle shows that there exists an energy functional of the charge density E[n],

$E[n] = \int v_{ext}(\mathbf{r})n(\mathbf{r})d\mathbf{r} + F[n]$ (2.2)

which attains its minimum if and only if the charge density n(r) is the exact ground-state density n(r). F[n] is a universal functional, independent of the external potential.

Kohn and Sham [15] proposed decomposing the functional according to :

$$F[n] = T_s[n(r)] + \frac{e^2}{2}\int drdr' \frac{n(r)n(r')}{|r-r'|} + E_{xc}[n(r)] \qquad (2.3)$$

where T is the kinetic energy of non-interacting electrons that possess the same density as the real interacting system. The second term is the Coulomb electronic repulsion. E_{xc} is the remaining correction known as the exchange-correlation energy. The minimization of this functional under the constraint of a given number of particles leads to the formally exact system of single-particle Kohn-Sham equations:

$$\left[-\frac{h^2}{2m}\nabla^2 + V_{eff}(r)\right]\Phi_i(r) = \varepsilon_i\Phi_i(r) \qquad (2.4)$$

where $V_{eff}(r) = v_{ext}(r) + e^2\int dr' \frac{n(r')}{|r-r'|} + \frac{\delta E_{ex}[n]}{\delta n(r)}$ (2.5)

and $n(r) = \sum_{i=1}^{N}|\Phi_i(r)|^2$ (2.5)

These equations describe a system of non-interacting particles in an effective potential $V_{eff}(r)$ at zero temperature. The effective potential consists of the external imposed potential $v_{ext}(r)$, the electrostatic Hartree interaction between the electrons and the exchange-correlation potential. The system must be solved self consistently, since the effective potential V_{eff} depends on the charge density n(r), which is in turn determined by the sum over the N wave functions of lowest energy. In practice, a guess for the charge density is taken as a starting point, from which a set of wave functions is determined by solving the one-particle Schrodinger equation. A new charge density is thus obtained and the process repeats until convergence is reached, as shown in figure 2.1. When the self-consistent charge density is known, the ions can be optionally relaxed to their equilibrium positions, using forces obtained for each configuration.

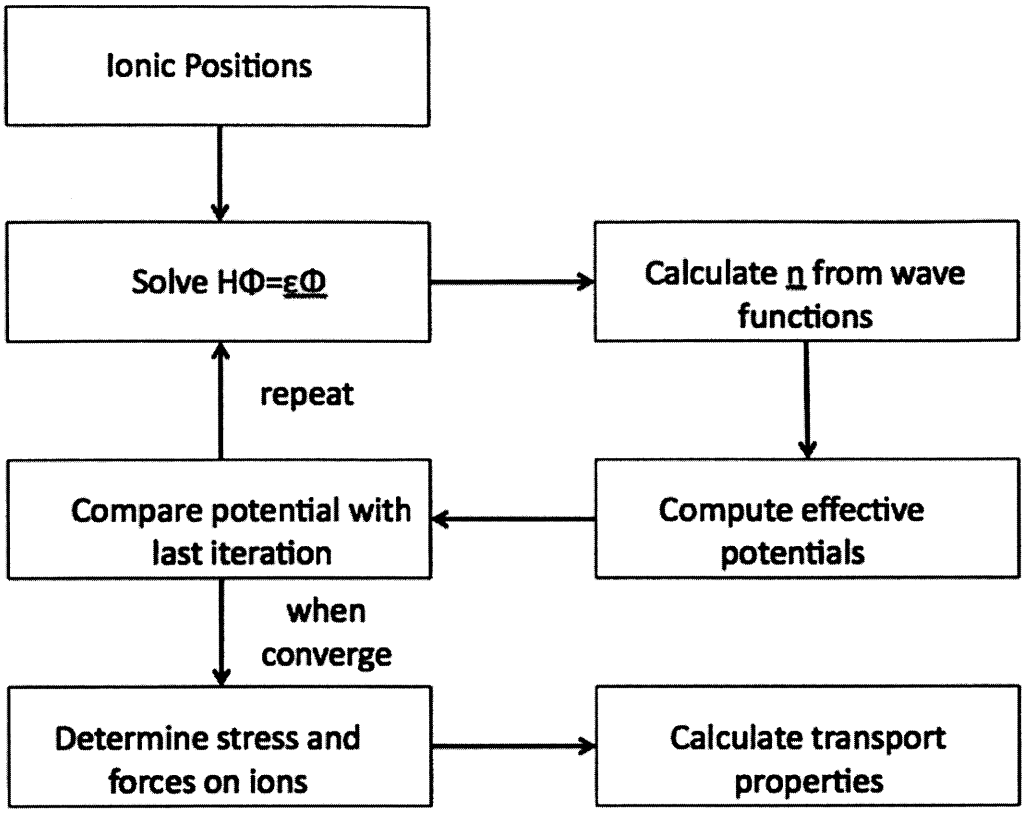

Figure 2.1 Self-consistent Calculations Flow Chart

In principle, the eigenvalues c_i of the Kohn-Sham equations do not have a physical significance, since they enter the formalism as Lagrange parameters to ensure orthogonality between the wave functions. However, it has become standard practice to interpret the c_i as estimates of the excitation energies because of the lack of simple alternative and its empirical justification [13].

2.3 Local Density Approximation

The exchange-correlation potential in equation (2.3) still needs to be defined in order to specify the problem completely. This can only be done approximately since the energy functional F[n] is not generally known. The approximation most generally used is the local density approximation (LDA), which exploits the knowledge of the exchange and correlation energy $E_{xc}(n)$ of a homogeneous electron gas of density n that has been obtained from alternative theoretical methods [13]. In this work, we use the parameterization of $E_{xc}(n)$ provided by Perdew and Zunger [16], as implemented in the Quantum Espresso package [30].

2.4 Pseudopotentials

In equation (2.4), v_{ext} is the imposed external all-electron potential. It is the Coulombic potential term for all electrons in the system. The deep core-electron wave functions are tightly bound to the nuclei and their spatial distribution remains essentially unchanged from one chemical environment to another, On the contrary, the valence electrons are higher in energy and are strongly influenced by the neighboring atoms. This insight has lead to the development of pseudopotentials, which is an effective potential constructed to replace the Coulombic potential such that core electrons are eliminated and only the valence electrons are described by pseudo-wavefunctions [17]. This pseudopotential approximation allows us to only treat active valence electrons explicitly while

considering core electrons frozen together with the nuclei. There are several different schemes for constructing pseudopotentials, including norm-conserving pseudopotentials [18] and ultrasoft pseudopotentials [19]. For our investigations we use ultrasoft pseudopotentials together with the LDA approximation.

2.5 BoltzTraP

BoltzTraP is a code package for calculation of the semi-classic transport coefficients created by Madsen and Singh [20]. It first expands the band energies using a smoothed Fourier expansion where the space group symmetry is maintained. Then it calculates transport properties with the analytical representation of the bands based on Boltzmann theory. Transport properties including electrical conductivity and Seebeck coefficient are calculated with the constant relaxation time approximation. This code package has been used successfully on several applications including the transport coefficients of intermetallic compounds, high TC superconductors and thermoelectric materials [21-23].

The Boltzmann equation describes the change of carrier distribution function induced by external fields, lattice phonon scattering, or various kinds of defect scattering. The various carrier scattering mechanisms are too complex to obtain an exact solution of the Boltzmann equation. So relaxation time approximation is

used here. Constant relaxation time approximation takes the relaxation time τ as independent of energy at fixed temperature and doping level. With this approximation, the Seebeck coefficient S and the electrical conductivity σ can be expressed as shown in equation (2.7) and (2.8) [29]

$$\sigma = e^2 \int d\varepsilon \left(-\frac{\partial f_0}{\partial \varepsilon}\right) \sum_k \tau \overline{v_k v_k} \delta(\varepsilon - \varepsilon_k) \qquad (2.7)$$

$$S = e k_B \sigma^{-1} \int d\varepsilon \left(-\frac{\partial f_0}{\partial \varepsilon}\right) \sum_k \tau \overline{v_k v_k} \delta(\varepsilon - \varepsilon_k) \frac{\varepsilon - \mu}{k_B T} \qquad (2.8)$$

where μ is the chemical potential, e is the electronic charge, τ is the relaxation time, f_0 is the Fermi function, $\overline{v_k}$ is the group velocity, and $\delta(\varepsilon-\varepsilon_k)$ is the delta function. This formalism has been used on a number of successful investigations of thermoelectric materials [24-28].

2.6 Quantum ESPRESSO

Quantum ESPRESSO [30] is a full ab-initio package implementing electronic structure calculation and materials modeling. It is based on density functional theory, plane waves and pseudopotentials. As an open source project released under GNU General Public License, it has been improved consistently in its efficiency, parallel architecture and user friendliness. It is one of the most popular ad initio calculation tools among material modeling groups worldwide.

2.7 Methodology Used in This Paper

For this study, we perform calculations on crystal structures, electronic structures and transport properties on filled and unfilled ternary skutterudites. Crystal structures, electronic structures and vibrational spectra are calculated using density-functional theory and density-functional perturbation theory with Quantum ESPRESSO with local density approximation functionals. Transport properties, including Seebeck coefficient and electrical conductivity are calculated with the BoltzTraP code package.

For each compound, a full variable cell relaxation is first performed using the Broyden-Fletcher-Goldfarb-Shanno [31] method until the force on each atom is smaller than 1e-4 Ry/bohr and the stress over the structure is less than 0.5 Kbar. Then a self-consistent field (SCF) calculation is performed on the relaxed structure to obtain the ground-state electron density on a 6*6*6 k-point grid. This electron density is used as an input for a non-self-consistent (NSCF) calculation to obtain the electronic structure on a 16*16*16 k-point grid. These steps are necessary in order to have smooth highly resolved electronic bands that can be processed using the BoltzTraP code. Both calculations use a cutoff energy of 30Ry. We use both SCF calculation and NSCF calculation with different k-point grids to reduce the calculation time. The projected density of states (PDOS) for each atom is obtained using the projwfc.x code within Quantum ESPRESSO.

Finally, transport properties are calculated with BoltzTraP using the relaxed crystal structure and band energies with constant relaxation time approximation.

Chapter 3: Calculations and Results

3.1 Skutterudites

A skutterudite is a mineral of the prototypical composition $CoAs_3$, which was named after the region where it was first found in southern Norway [32]. The ideal skutterudite crystal structure belongs to space group Im-3. It can be viewed as a corner sharing network of heavily titled pnictogen octahedra with a transition metal, typically Co, in the center. One great feature of the skutterudite structure is that it contains two large empty cages, or voids, per unit cell, which can be partially or completely filled with filler atoms.

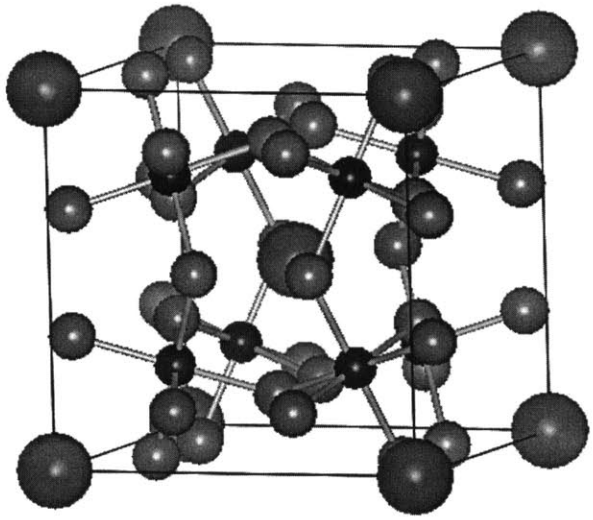

Figure 3.1 Crystal structure of filled skutterudites. Transition metals, pnictogens, and fillers are presented as blue, khaki, and green spheres, respectively. Visualized with VESTA [33].

Skutterudites were identified as promising thermoelectric material about 20 years ago [34] when people discovered the remarkable feature of the fillers. By filling the voids in skutterudites, their lattice thermal conductivities can be reduced dramatically. The commonly cited reason [35] for this reduction in thermal conductivity is that the rattling motion of the filler atoms effectively scatters heat-carrying phonons and thus reduces the lattice contribution to the thermal conductivity. Experiments [36, 37] have also shown that the filler atoms are weakly bound to the cage and rattle about their equilibrium position.

Combined with good electronic properties, low thermal conductivity makes the filled skutterudite a potential candidate for thermoelectric applications. With the increasing interest in thermoelectric materials, research has been done on a large variety of filler atoms, including La, Ce, Pr, Nd, Sm, Eu, Yb, Ba, Sr, Ca, Ge, Sn, Pb, Tl, U, Th, etc. [38]. Some doped Skutterudites have shown exceptionally high ZT values at elevated temperatures. $CoSb_3$-based skutterudites with ZT values approaching 1.4 around 800K have been reported recently [39].

3.2 Ternary Skutterudites

In addition to binary skutterudites, which are compounds with composition MX_3, another group of skutterudite-related materials, ternary skutterudites, also exists. Ternary skutterudites can be obtained by an isoelectronic replacement of

pnictogen atoms with the atoms from group 14 and 16 of the periodic table. They have a general formula $MY_{1.5}Ch_{1.5}$, where Y and Ch are elements from ground 14 and 16, for example $CoGe_{1.5}Te_{1.5}$.

A number of ternary skutterudites [40-45], including $CoGe_{1.5}Te_{1.5}$, $CoSn_{1.5}Se_{1.5}$, $CoSn_{1.5}Te_{1.5}$ and $CoGe_{1.5}S_{1.5}$,have been reported in the last few decades. Ternary skutterudites are isoelectronic to the binary skutterudites. But studies on $CoGe_{1.5}S_{1.5}$ [40] and $CoGe_{1.5}Se_{1.5}$ [45] suggest that these compounds have a modified skutterudite structure with lower symmetry from cubic to rhombohedral.

Although a number of ternary skutterudites have been reported, most work to date is only done on unfilled ternary skutterudites with focus on their synthesis and structural properties. Because ternary skutterudites share similar crystal and electronic structures with binary skutterudites, we can expect their behavior to be similar. Unfilled ternary skutterudites have been shown to have low thermal conductivity. Laufek et al. [45] found the thermal conductivity of $CoSn_{1.5}Se_{1.5}$ sample is about two times lower than that of similar prepared $CoSb_3$. Filling them may reduce their thermal conductivity even more, resulting in potential good thermoelectric materials with high ZT values. In this work, we use an ab initio approach to study the electronic and transport properties of filled and unfilled ternary skutterudites. The aim is to give a theoretical interpretation of some experimenta' results and provide theoretical data on their transport properties,

which can be used to evaluate their potential as thermoelectric materials in certain applications.

3.3 Calculation Result of Unfilled Ternary Skutterudites

In this part, we show calculation results for ternary skutterudites $CoGe_{1.5}Te_{1.5}$, $CoGe_{1.5}Se_{1.5}$, $CoGe_{1.5}S_{1.5}$, $CoSn_{1.5}S_{1.5}$, $CoSn_{1.5}Se_{1.5}$, and $CoSn_{1.5}Te_{1.5}$. The initial structures of those compounds are obtained though substituting antimony in $CoSb_3$ with elements from group 14 and 16.

3.3.1 Structure

To investigate the effect of substitution on crystal structure, a full variable cell relaxation is performed using the BFGS method on each compound. The resulting structure of $CoGe_{1.5}S_{1.5}$ is shown below in figure 3.2. It belongs to the rhombohedral lattice system with lattice parameter a=b=c=7.888Å and alpha=beta=gamma=89.89. This symmetry change is consistent with experiment result measured by Vaqueiro et al [46].

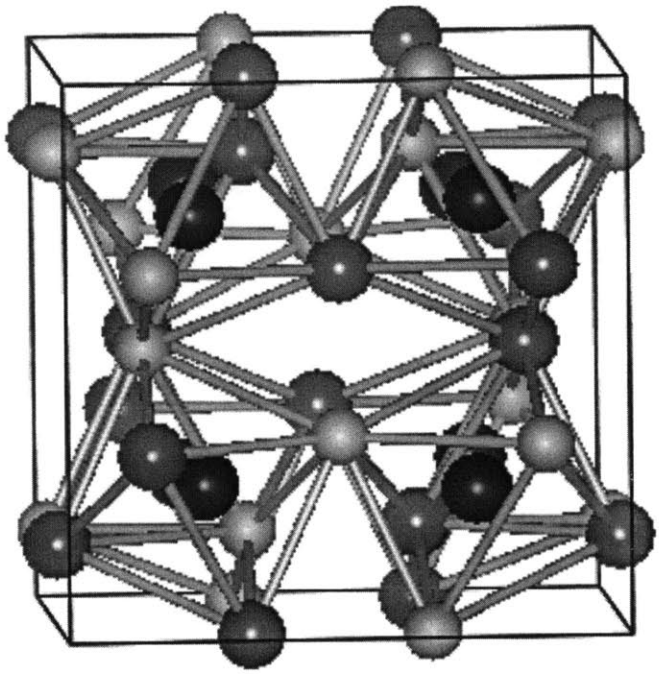

Figure 3.2 Structure of relaxed $CoGe_{1.5}S_{1.5}$. Co, Ge, and S atoms are presented as blue, grey, and yellow spheres, respectively. Visualized with VESTA [33].

Our computed structural parameters are listed in table 3.1 below. The equilibrium lattice parameter a0 of each compound is plotted in figure 3.3. This data shows a strong correlation between the lattice parameter and the size of the substitution atoms. The lattice parameter increases with larger substitution atoms. In all three $CoGe_{1.5}(S, Se, Te)_{1.5}$, $CoGe_{1.5}S_{1.5}$ has the smallest lattice size while $CoGe_{1.5}Te_{1.5}$ has the largest. In all three $CoSn_{1.5}(S, Se, Te)_{1.5}$, $CoSn_{1.5}S_{1.5}$ has the smallest lattice size while $CoSn_{1.5}Te_{1.5}$ has the largest. A similar trend also appears in the other substitution site. For example, the lattice parameter of $CoSn_{1.5}Te_{1.5}$ is larger than that of $CoGe_{1.5}Te_{1.5}$.

Table 3.1 Crystal structure of PSTS CoY1.5Ch1.5 after relaxation of all internal degrees of freedom. The symmetry is $R\bar{3}$(space group 148)

	$CoGe_{1.5}S_{1.5}$	$CoGe_{1.5}Se_{1.5}$	$CoGe_{1.5}Te_{1.5}$	$CoSn_{1.5}S_{1.5}$	$CoSn_{1.5}Se_{1.5}$	$CoSn_{1.5}Te_{1.5}$
a_L (Å)	7.888	8.186	8.622	8.311	8.610	9.023
α (deg)	89.90	89.83	89.95	89.87	89.98	89.97
Co (2c) x	0.258	0.251	0.243	0.267	0.260	0.253
Co (6f) x	0.258	0.253	0.249	0.262	0.260	0.255
Co (6f) y	0.762	0.753	0.745	0.773	0.764	0.756
Co (6f) z	0.754	0.752	0.747	0.778	0.755	0.751
Y_A (6f) x	0.999	0.998	0.996	0.001	0.999	0.998
Y_A (6f) y	0.335	0.327	0.318	0.333	0.328	1.321
Y_A (6f) z	0.151	0.158	0.167	0.149	0.156	0.165
Y_B (6f) x	0.499	0.500	0.501	0.499	0.500	0.501
Y_B (6f) y	0.835	0.827	0.818	0.834	0.828	0.821
Y_B (6f) z	0.349	0.341	0.332	0.351	0.343	0.335
Ch_A (6f) x	0.000	0.00	0.999	0.001	0.001	0.000
Ch_A (6f) y	0.344	0.344	0.345	0.337	0.328	0.339
Ch_A (6f) z	0.849	0.850	0.851	0.840	0.843	0.845
Ch_B (6f) x	0.502	0.503	0.505	0.501	0.502	0.503
Ch_B (6f) y	0.844	0.844	0.845	0.837	0.838	0.839
Ch_B (6f) z	0.650	0.649	0.648	0.659	0.657	0.655

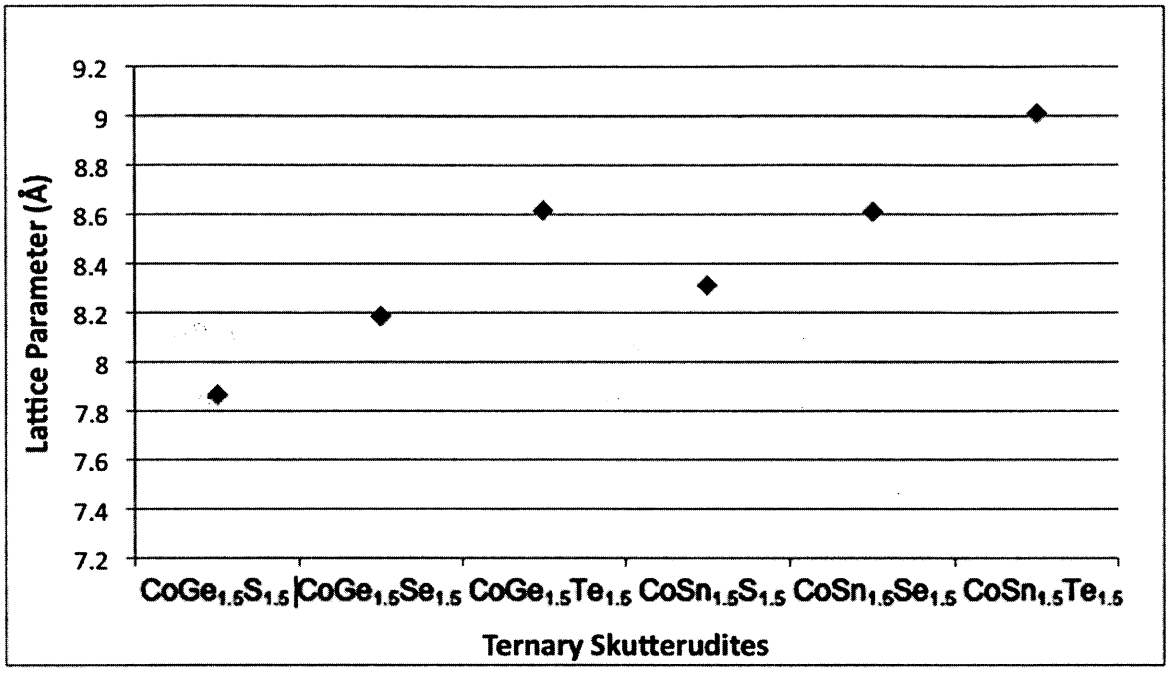

Figure 3.3 Lattice parameters for relaxed unfilled ternary skutterudites.

3.3.2 Density of States

The total and projected density of states (PDOS) of each atom in some ternary skutterudites is calculated and shown in figures 3.4 and 3.5 below. In these figures, energy in eV (horizontal axis) is plotted vs. electrons/eV (horizontal axis); the solid line represents the total DOS, while the dashed lines are projected DOS for each atom. It is good to note that each orbital of each atom had been projected separately in order to find the total contribution attributed from each atom.

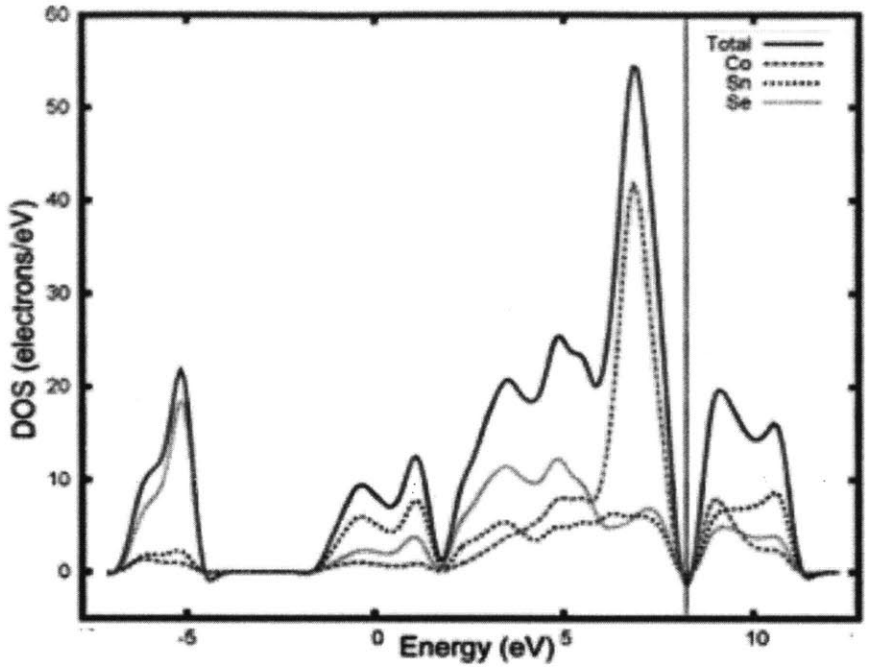

Figure 3.4 PDOS of $CoSn_{1.5}Se_{1.5}$. The Fermi level is marked with a grey line.

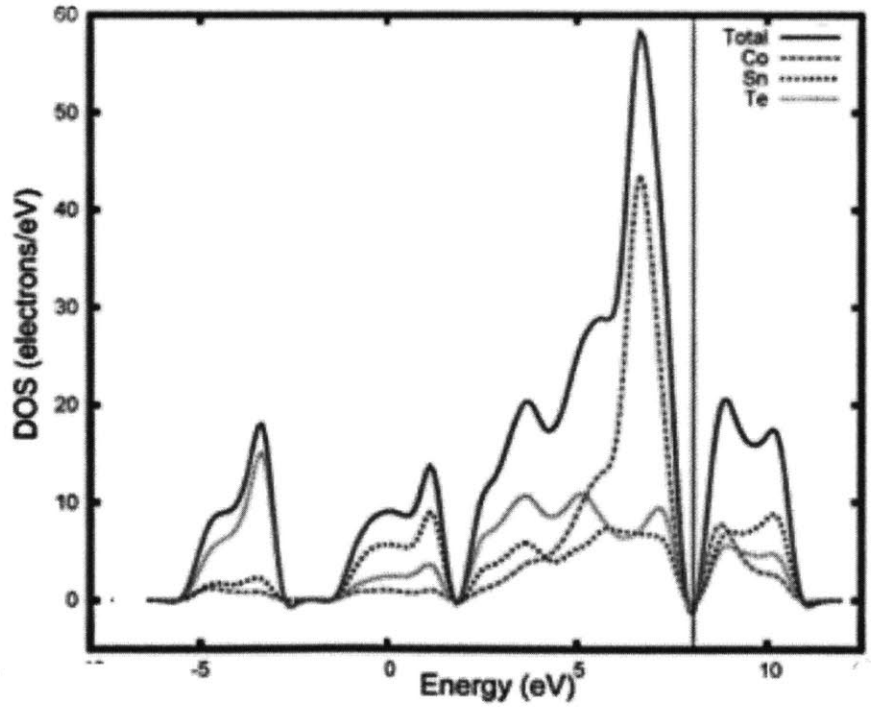

Figure 3.5 PDOS of $CoSn_{1.5}Te_{1.5}$. The Fermi level is marked with a grey line.

From figure 3.4 and 3.5, we see that there are two distinct ranges in the electronic DOS separated from each other by energy gaps. The conduction band is primarily formed by a mixture of all orbitals, while the valence band close to the Fermi level mainly consists of Co states. Generally, the electrical conductivity and the Seebeck coefficient of a material are mainly determined by the DOS near the Fermi level.

3.3.3 Transport Properties

Starting from the band structures, we can estimate transport properties using a semi classical Boltzmann transport approach with the constant relaxation time approximation. A summary of the Seebeck coefficient of each ternary skutterudites is shown in figure 3.6. The Seebeck coefficients are plotted against chemical potential , which is the shifted Fermi level at different carrier concentration. The solid black line represents $CoSb_3$. Comparing $CoSb_3$ and ternary skutterudites, we can see that the Seebeck coefficients of ternary skutterudites are better than that of $CoSb_3$. This finding is consistent with the experimental results on $CoSn_{1.4}Te_{1.5}$ [46].

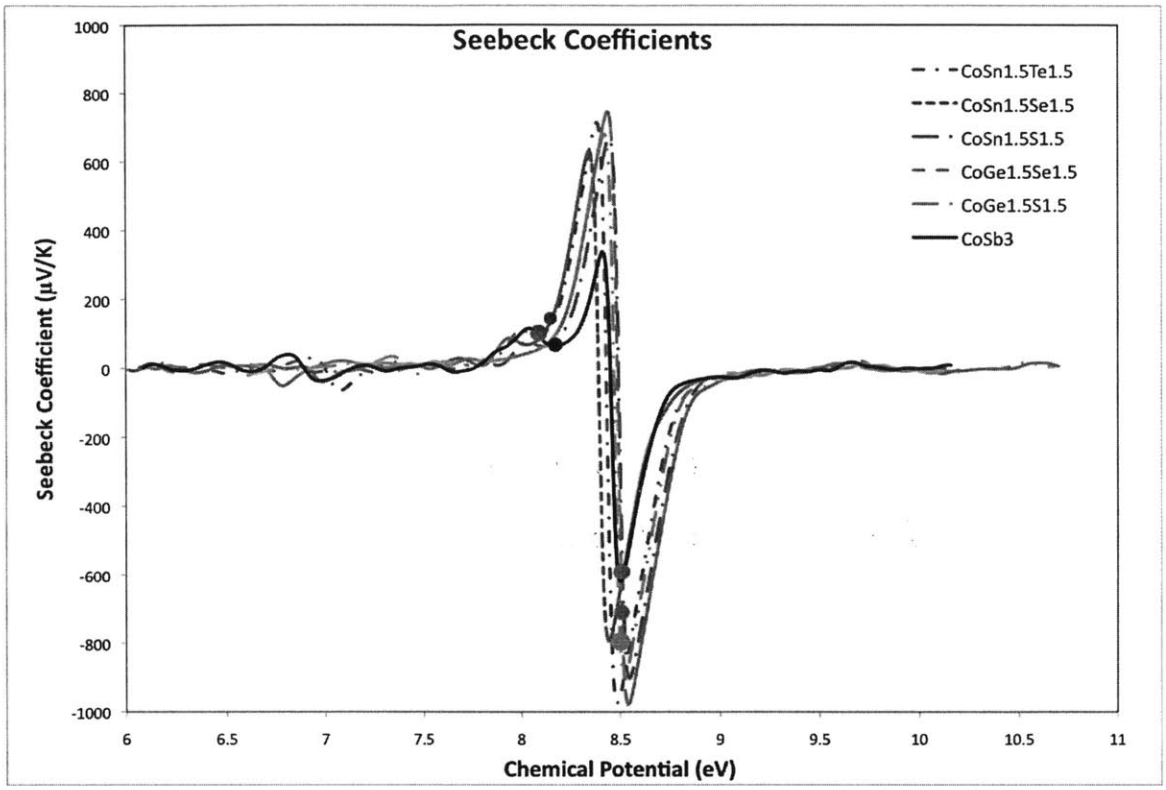

Figure 3.6 Seebeck coefficients of ternary skutterudites at 500K. The intrinsic Fermi level of each compound is marked with a solid dot on its curve.

The electrical conductivities are computed with a constant relaxation time of 10^{-14} s, which is a typical value in semiconductors that reproduces many experimental measurements [47]. The calculation results are shown in figure 3.7. Within the constant relaxation time approximation, the Seebeck coefficient is independent of the value of the relaxation time. We note however that, unlike the Seebeck coefficient, the electrical resistivity is inversely proportional to the actual value of the relaxation time under the constant relaxation-time approximation. Comparing with the values of $CoSb_3$, which is shown as a black solid line on figure 3.7, the electrical conductivities of ternary Skutterudites are smaller than that of $CoSb_3$,

assuming the same value of the relaxation time. The values range up to one half of $CoSb_3$'s value. The low electrical conductivity is consistent with several experiment reports on $CoSn_{1.5}Se_{1.5}$ [48], although the exact mechanism of the electron scattering is not certain. Our computations show that assuming the same relaxation mechanisms, purely band structure effects result in reduced conductivity.

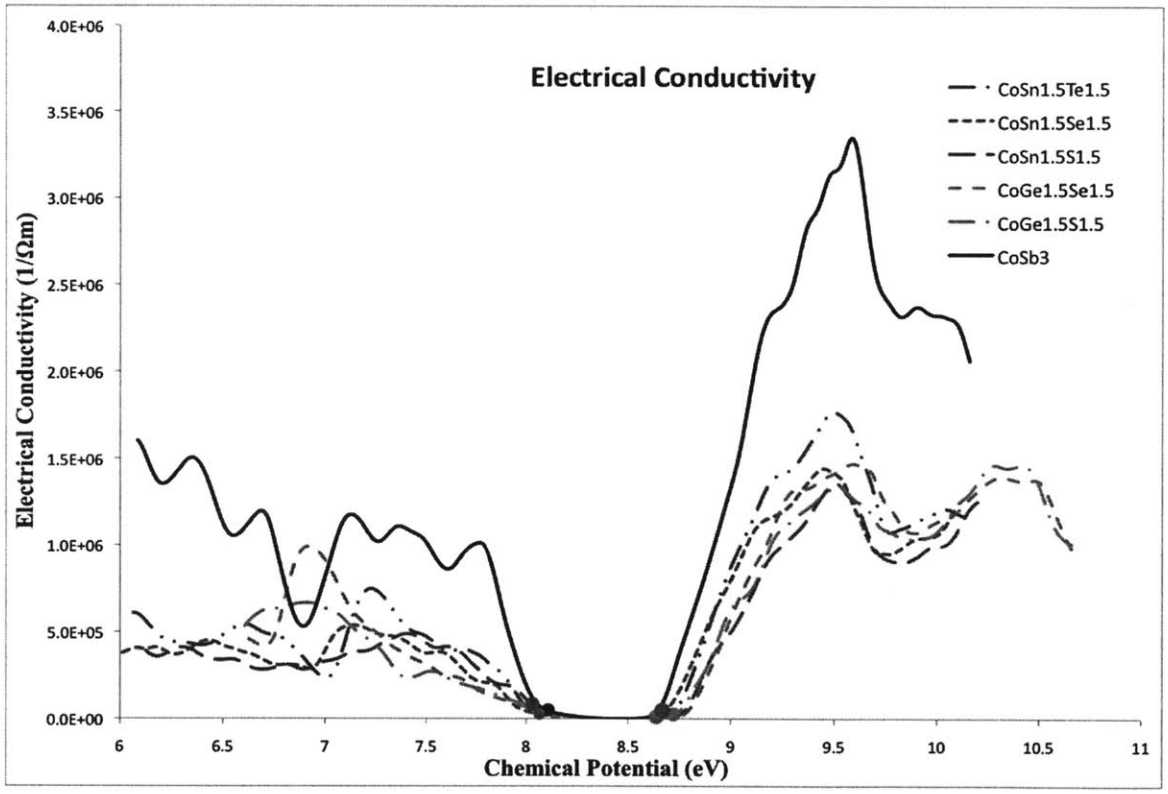

Figure 3.7 Electrical conductivities of ternary skutterudites at 500K. The intrinsic Fermi level of each compound is marked with a solid dot on its curve.

3.4 Calculation Results of Filled Ternary Skutterudites

Skutterudites have good potential as thermoelectric materials because their structures contain voids, which can be filled by other atoms. The filling atoms, called ratters, vibrate around their equilibrium positions and increase phonons scattering which in turn effectively reduces the thermal conductivity. The reduction of thermal conductivity can cause an improvement to the ZT value. In some cases, the filling of the voids in skutterudites does not only affect the lattice thermal conductivity but also the electronic transport properties. Thus when we investigate the properties of ternary skutterudites, we have a strong interest in filled ternary skutterudites, especially in the effects of filling on transport properties.

Alkaline-earth metals have been used in filling skutterudites for many years. One fact to note is that alkaline earths are inexpensive and much more available than heavy rare earths. David J. Singh [49] computationally investigated alkaline-earth-filled skutterudite antimonides and found high thermopower at high carrier concentrations. Because alkaline-earth-filled skutterudites have shown great improvement in their thermal properties, we start our study on filling ternary skutterudites with alkaline earths Ca, Ba and Sr. Besides alkaline earth, we also study filling with La on selected ternary skutterudites. Favorable thermoelectric properties are reported on La-filled binary skutterudites by D.J. Singh and I. I. Mazin [50].

Early studies have shown that for filled skutterudites, the largest decrease in the lattice thermal conductivity may not be found near 100% filling of the voids [51]. It is observed that a relatively small filling rate might result in a relatively large decrease in the lattice thermal conductivity. A point-defect-type phonon scattering effect from the partial, random distribution of filler atoms could be an explanation for this phenomena. To get a good understanding of the effect of void filling on ternary skutterudites, we calculate electronic and transport properties on both half-filled and fully-filled ternary skutterudites.

For half-filled ternary skutterudites, we use a 33-atom unit cell with one void filled. The filler atom is at the center of the unit cell, as shown in figure 3.8 (a). For fully-filled ternary skutterudites, we use a 34-atom unit cell with both voids filled. The filler atoms are at the center and corners of the unit cell, as shown in figure 3.8 (b). In both cases, the filler atoms occupy the same crystallographic sites in each cell resulting in total 6 symmetry operations of the unit cell. This situation is somewhat artificial, since it neglects any configurational disorder in real samples. But it is a good first step towards the understanding of partial and full filling in ternary skutterudites.

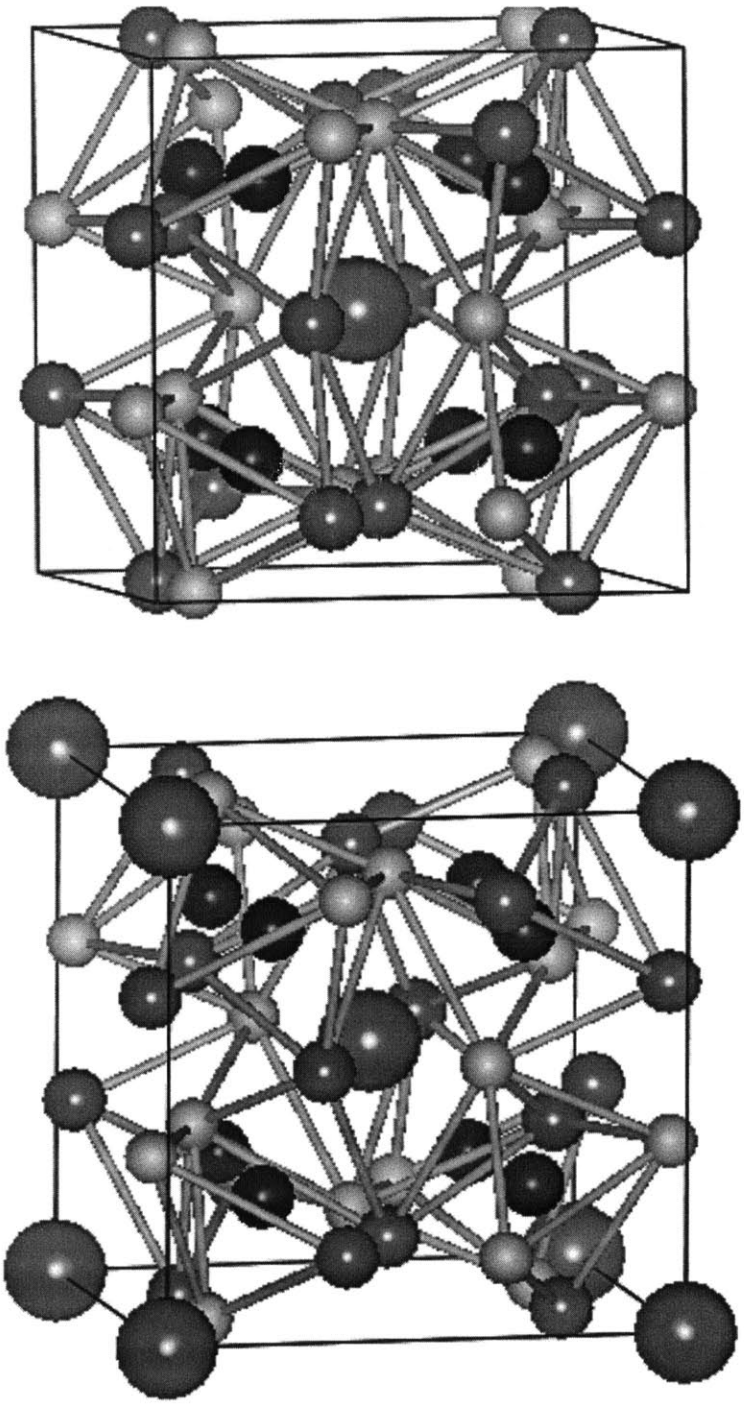

Figure 3.8 (a) Structure of $CaCo_8Ge_{12}S_{12}$ (b) Structure of $Ca_2Co_8Ge_{12}S_{12}$. Ca, Co, Ge, and S atoms are represented by light blue, dark blue, yellow, and grey spheres, respectively.

For all filled ternary skutterudites, crystal structures were first obtained from variable cell relaxation. Then electronic-structure calculations were performed with local density approximation of Perdew-Zunger (LDA) using Quantum ESPRESSO. At last, transport properties were calculated with BoltzTraP program making use of the constant relaxation time approximation. A summary of calculated filled ternary skutterudites is shown in table 3.2.

Table 3.2 Summary of calculated filled ternary skutterudites in this study.

	Ba	Ca	Sr	La
$CoGe_{1.5}S_{1.5}$	50%, 100%	50%, 100%		50%, 100%
$CoGe_{1.5}Se_{1.5}$	50%, 100%		50%, 100%	50%, 100%
$CoGe_{1.5}Te_{1.5}$	50%, 100%	50%, 100%	50%, 100%	50%, 100%
$CoSn_{1.5}S_{1.5}$	50%, 100%	50%, 100%		
$CoSn_{1.5}Se_{1.5}$	50%, 100%	50%, 100%		
$CoSn_{1.5}Te_{1.5}$	50%, 100%			

3.4.1 Structure

Full variable cell relaxation has been performed using the Broyden-Fletcher-Goldfarb-Shannomethod (BFGS) until the force on each atom becomes smaller than 1e-4 Ry/bohr and the stress over the structure is less than 0.5 Kbar. The results are presented in table 3.3, figure 3.9 and figure 3.10.

Table 3.3 Lattice parameters(Å) for filled ternary skutterudites.

	$CoGe_{1.5}S_{1.5}$	$CoGe_{1.5}Se_{1.5}$	$CoGe_{1.5}Te_{1.5}$
50% Ba filled	7.96162	8.27674	8.69020
100% Ba filled	8.04296	8.35600	8.76060
50% Ca filled	7.96330		8.69420
100% Ca filled	8.04991		8.76969
50% Sr filled		8.39989	8.84512
100% Sr filled		8.46851	8.91154
50% La filled	8.13799	8.40465	8.84973
100% La filled	8.21169	8.47645	8.91662
	$CoSn_{1.5}S_{1.5}$	$CoSn_{1.5}Se_{1.5}$	$CoSn_{1.5}Te_{1.5}$
50% Ba filled	8.39349	8.68680	9.07506
100% Ba filled	8.47057	8.76040	9.13993
50% Ca filled	8.39367	8.68775	
100% Ca filled	8.47298	8.76373	

Comparing the values in table 3.3 with table 3.1, we can see that the lattice sizes have about 10% differences between the filled and unfilled ternary skutterudites. From previous study of $CoSb_3$, we know that this amount of structure change might bring large change to the electronic structures. We also see the lattice parameters increase with filling ratio for each ternary skutterudite. Figure 3.9 plots the lattice parameter versus the filling ratio. This is consistent with others' observation [52]. Figure 3.10 plots the lattice parameters versus the filling atoms. It shows that La filled ternaries have the largest size while the Ba filled ones, surprisingly, have the smallest size.

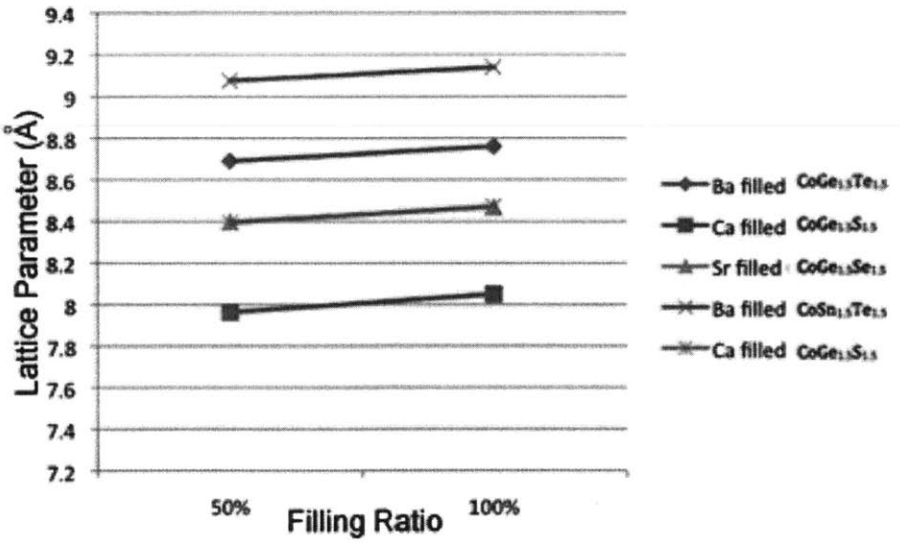

Figure 3.9 Lattice parameters (Å)vs filling ration

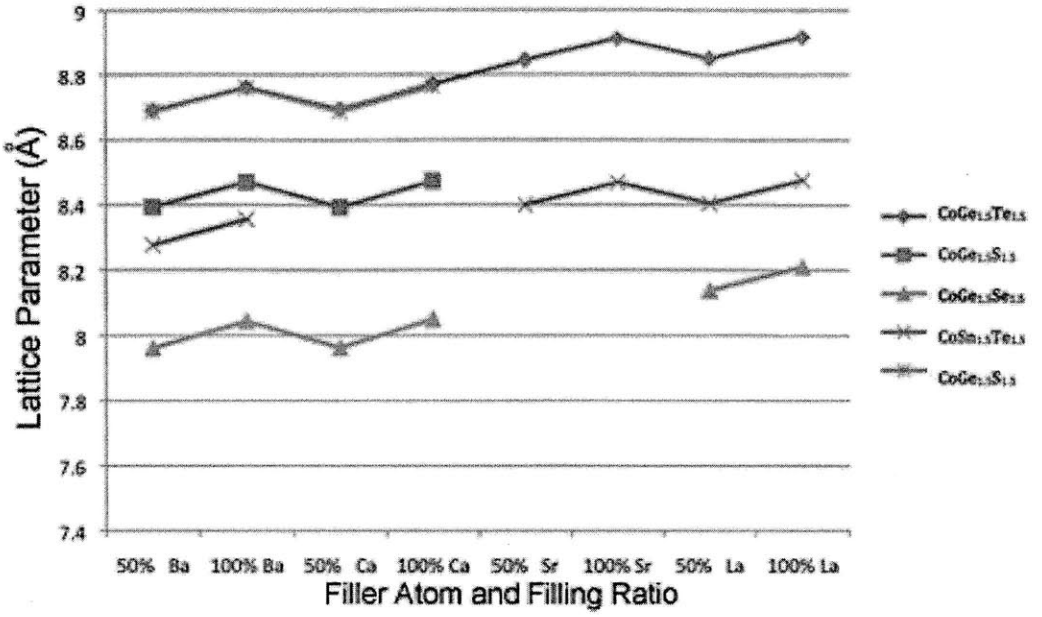

Figure3.10 Lattice parameter (Å) vs filling atoms

3.4.2 Density of States

The total and projected density of states (PDOS) of each atom in filled ternary skutterudites is calculated using ab initio methods and shown in figure 3.11. In these figures, energy in eV (horizontal axis) is plotted vs electrons/eV (horizontal axis); the solid line represents the total DOS, while the dashed lines are projected DOS for each atom. The total contribution of each atom is calculated from the PDOS of each orbital.

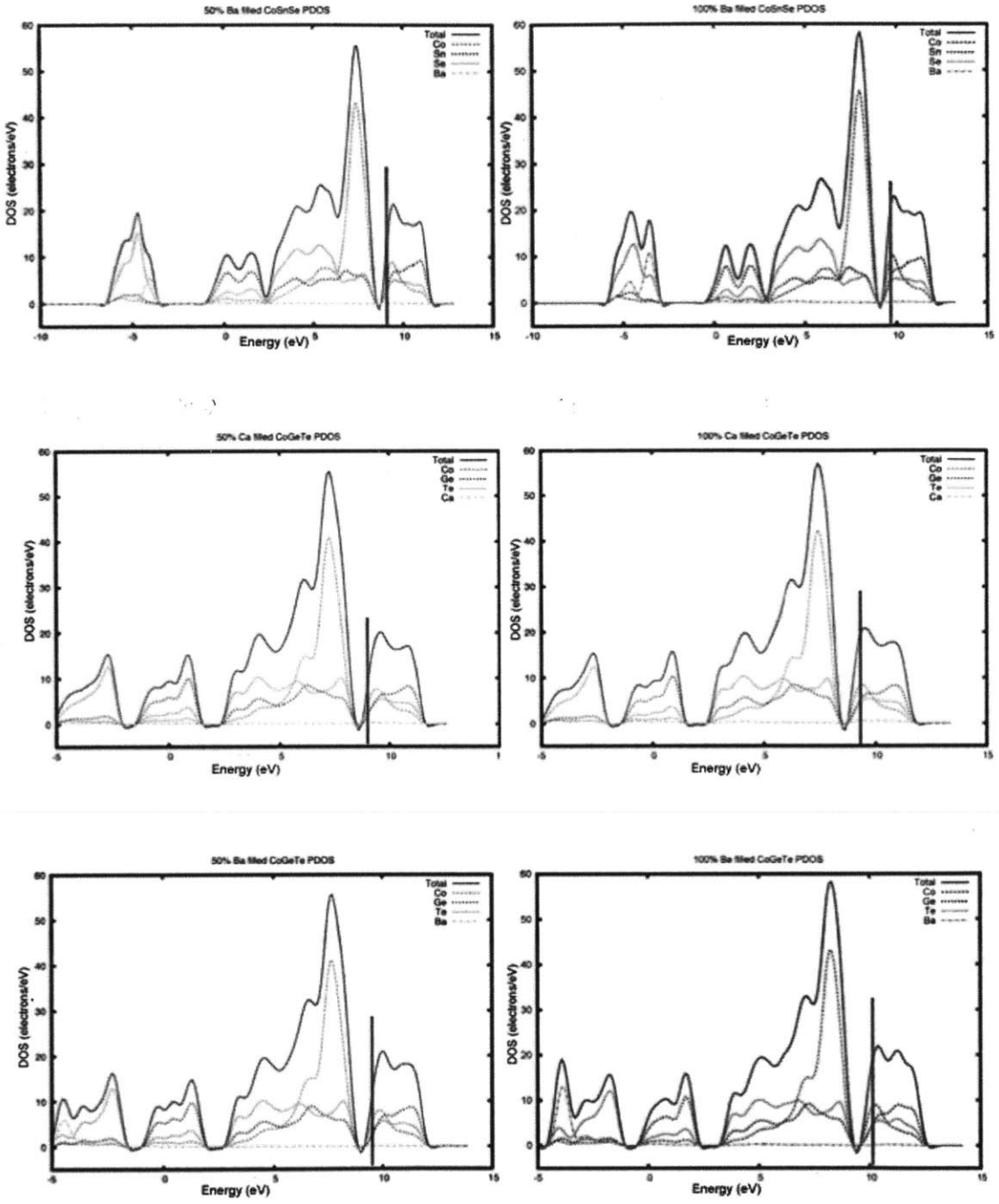

Figure 3.11 Calculated PDOS of Ba and Ca filled skutterudites $CoGe_{1.5}Te_{1.5}$ and $CoSn_{1.5}Se_{1.5}$. The Fermi level is marked with a grey line.

The PDOS shows that the states of filler atoms, Ba and Ca, are low in energy. Because those states are far from the band gap, they may have little effect on the band gap. But they have effect on the Fermi levels. Comparing with figure 3.4 and 3.5, we can see that filling shifts the Fermi level in these ternary skutterudites.

3.4.3 Transport Properties

Electrical conductivity of each filled ternary skutterudites is plotted in figure 3.12. The solid black line represents the electrical conductivity of $CoSb_3$. All calculations are done under the assumption of constant relaxation time. The calculations show a relatively low electrical conductivity of filled ternary skutterudites. This is consistent with our calculation on unfilled ternary skutterudites. Comparing filled and unfilled ternary skutterudites, we see that filling does not have a large effect on electrical conductivity for most ternary skutterudites.

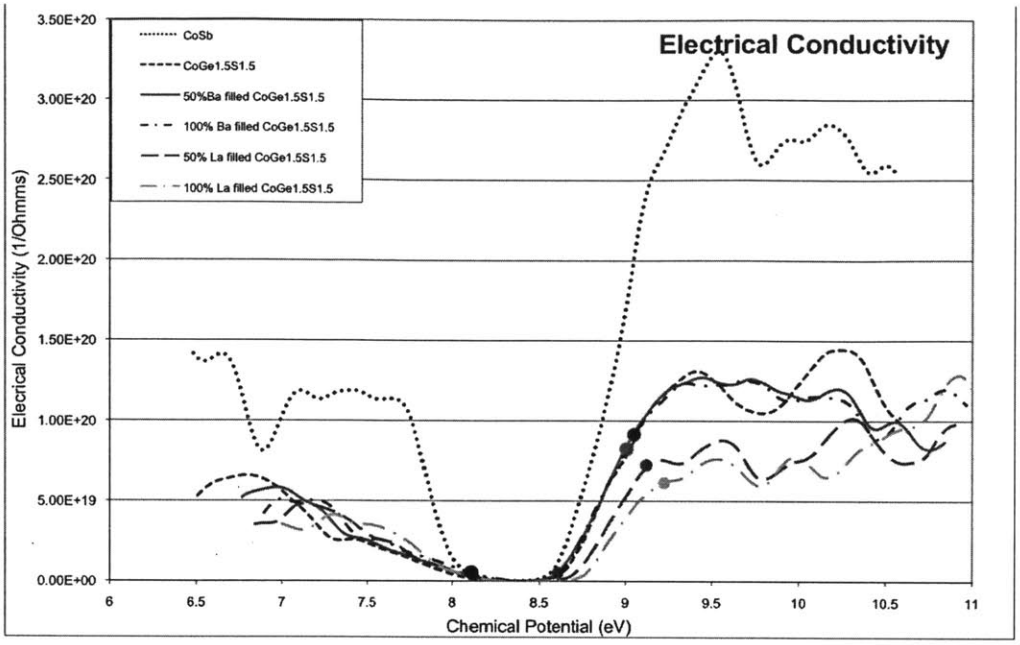

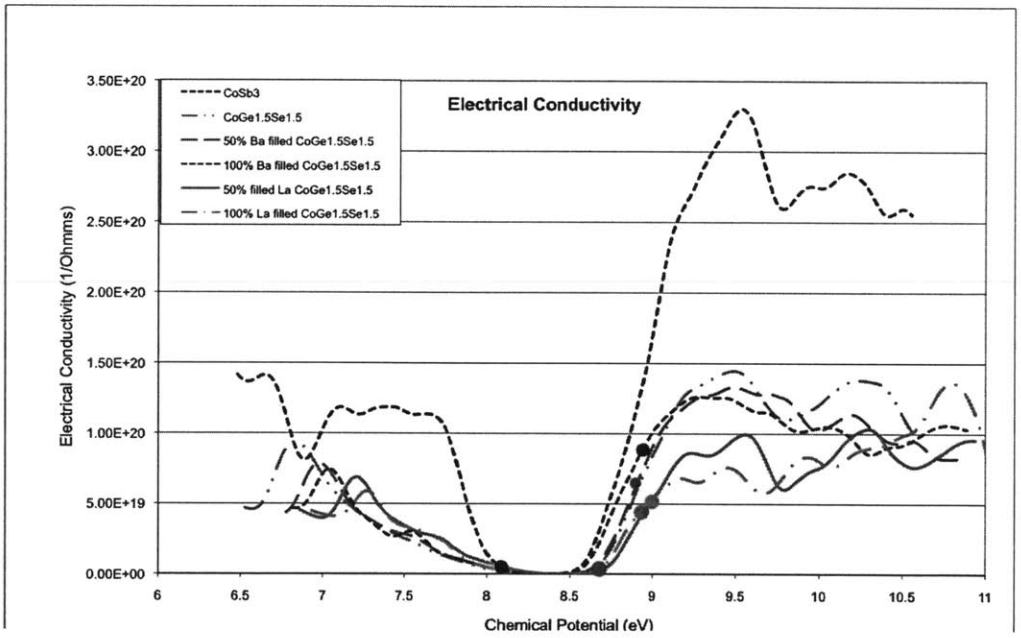

Figure 3.12 Electrical conductivities of filled ternary skutterudites, $CoGe_{1.5}S_{1.5}$ and $CoGe_{1.5}Se_{1.5}$ at 500K. The intrinsic Fermi level of each compound is marked with a solid dot on its curve.

Calculated Seebeck coefficients are plotted in figure 3.13 and figure 3.14. The black solid line represents $CoSb_3$. From the comparison of filled and unfilled ternary skutterudites, we can see that Seebeck coefficients are lower in alkaline-earth filled ones but still higher than that of $CoSb_3$, especially in the p-type region. La filled Skutterudites have better Seebeck coefficients than unfilled ones.

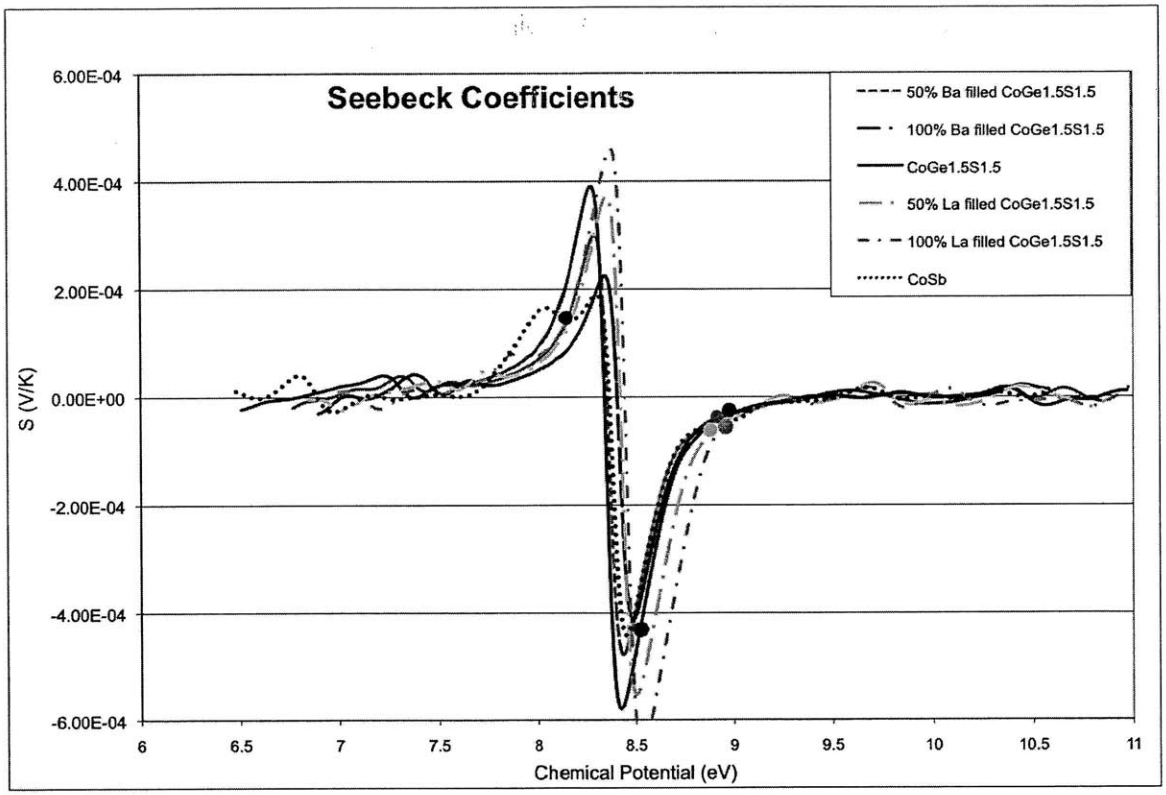

Figure 3.13 Seebeck coefficients of filled $CoGe_{1.5}Se_{1.5}$ at 500K . The intrinsic Fermi level of each compound is marked with a solid dot on its curve.

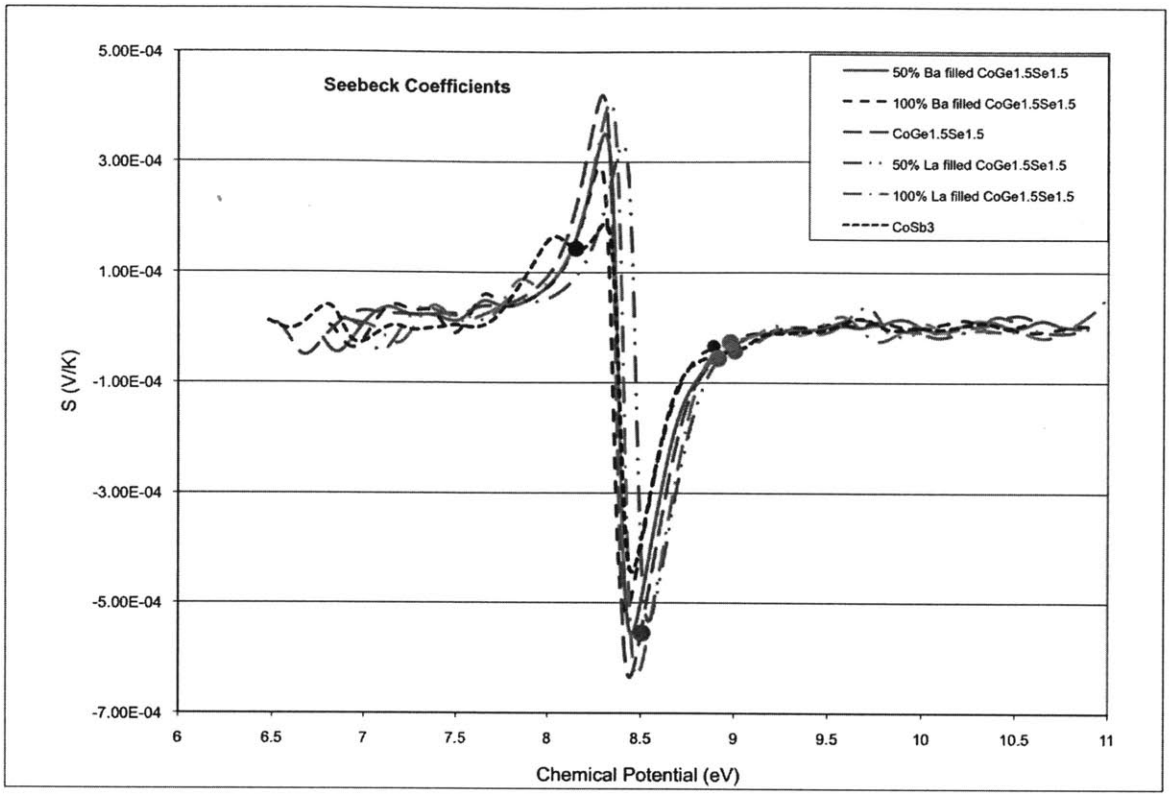

Figure 3.14 Seebeck coefficients of filled $CoGe_{1.5}Se_{1.5}$ at 500K . The intrinsic Fermi level of each compound is marked with a solid dot on its curve.

Chapter 4: Discussion

4.1 Potential as Thermoelectric Materials

One of the main purposes of this study is to address the potential of filled and unfilled ternary skutterudites as thermoelectric materials. In this part, we are going to have a deep look into its transport properties including electrical conductivities, Seebeck coefficients, power factor, and ZT value.

4.1.1 Electrical Conductivity and Power Factor

One disadvantage of ternary skutterudites we can see from our calculations is that they all have relatively low electrical conductivity compared with other popular skutterudites such as $CoSb_3$. For example, the electrical conductivity of unfilled $CoSn_{1.5}Te_{1.5}$ is only as half as that of $CoSb_3$ under the assumption of same constant relaxation time.

This low electrical conductivity is also reported from several experiments. Vaqueiro et al. [46] found high resistivity on $CoGe_{1.5}S_{1.5}$ and $CoGe_{1.5}Te_{1.5}$. Laufek et al. [48] discovered similar high resistivity on $CoSn_{1.5}Se_{1.5}$. One possible explanation of the low electrical conductivity is that their charge-carriers have low mobility. As it has been argued that in materials containing elements with

different electronegativities, charge fluctuations from atom to atom increase the charge-carrier scattering and thus decrease their mobility [53].

Since ternary skutterudites have low electrical conductivities and high Seebeck coefficients, their power factor, $S^2\sigma$ become a crucial parameter in determining their potential as TE materials. Figure 4.1 and 4.2 show the power factor of some unfilled and filled ternary skutterudites at 500K. We should note that the value of the calculated power factor is related to our assumption of the constant relaxation time.

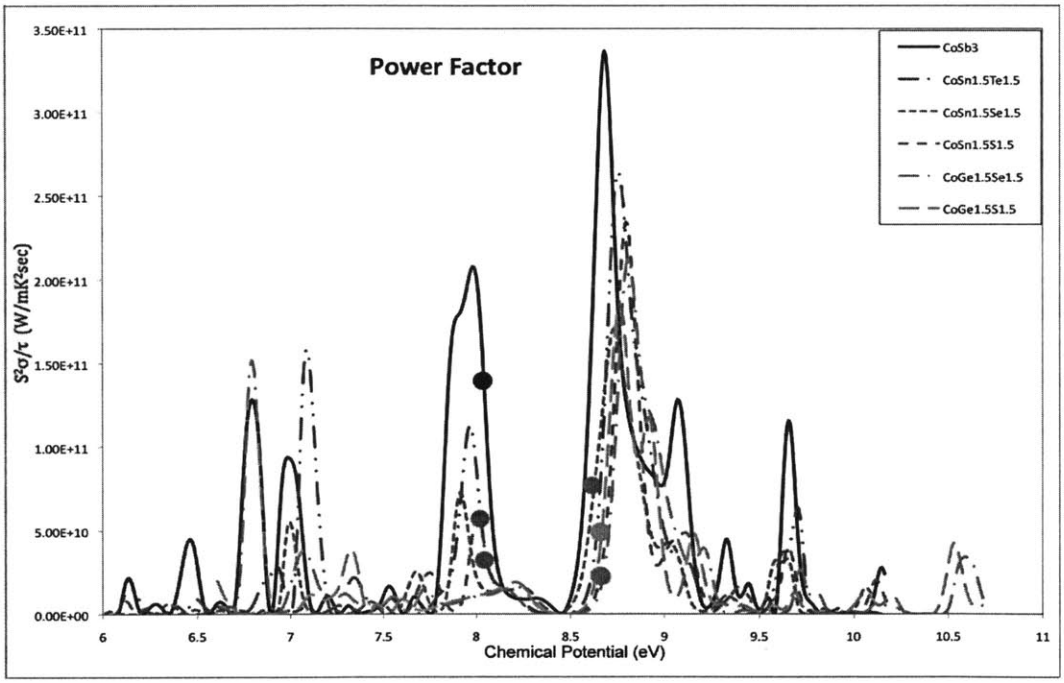

Figure 4.1 Power Factor with respect to relaxation time $S^2\sigma/\tau$ of unfilled ternary skutterudites at 500K. The intrinsic Fermi level of each compound is marked with a solid dot on its curve. One obtains the power factor in the units of $W/(mK^2)$ by multiplying by τ in units of second.

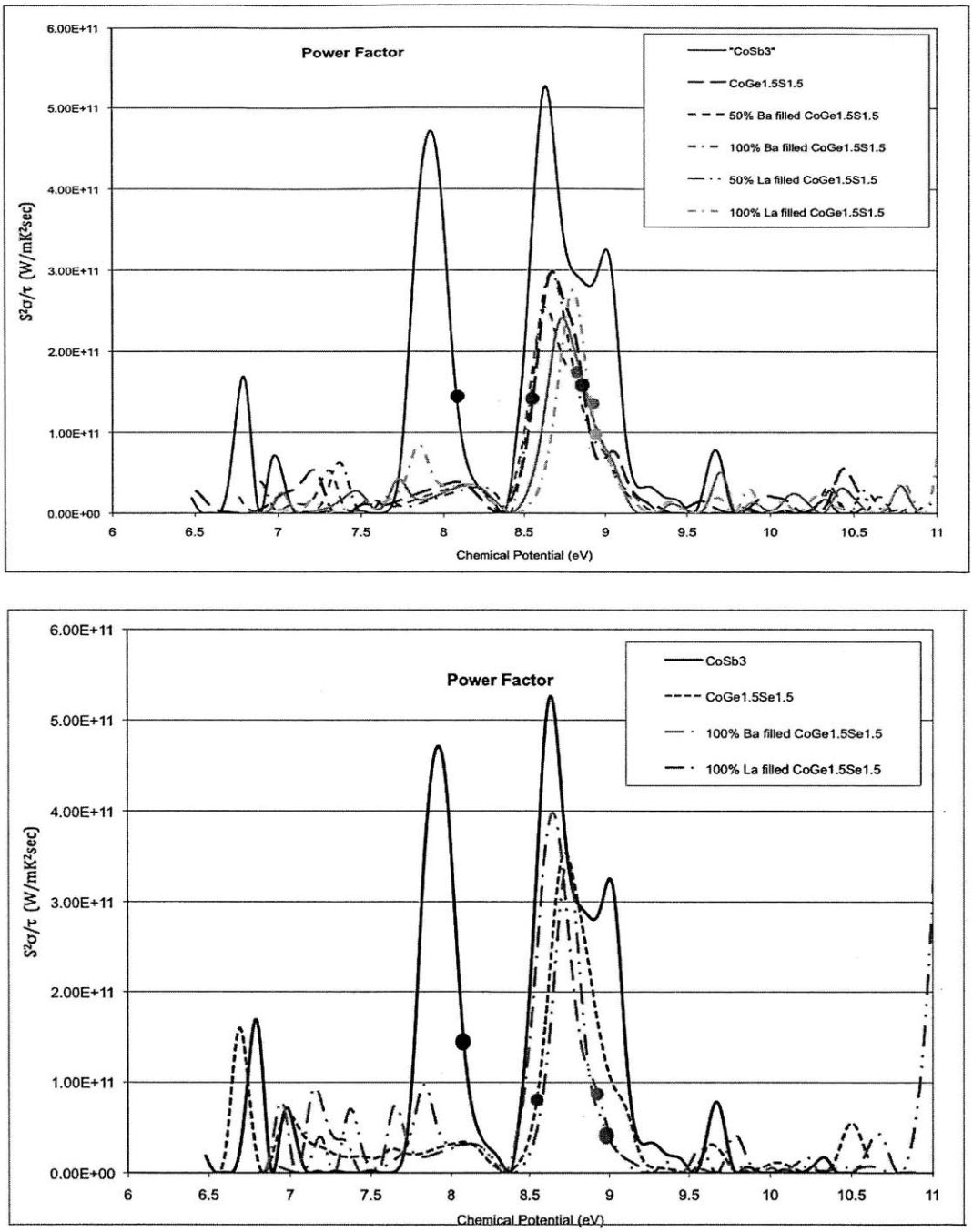

Figure 4.2 Power Factor with respect to relaxation time $S^2\sigma/\tau$ of filled $CoGe_{1.5}S_{1.5}$, and filled $CoGe_{1.5}Se_{1.5}$ at 500K. The intrinsic Fermi level of each compound is marked with a solid dot on its curve. One obtains the power factor in the units of $W/(mK^2)$ by multiplying by τ in units of second.

Comparing the transport properties of ternary skutterudites with CoSb3, we can see a trade off between Seebeck coefficient and electrical conductivity. While ternary skutterudites have better Seebeck coefficients, their electrical conductivities are lower. This trade-off is often seen on thermoelectric materials and limits their ZT value[56, 57]. As shown in figure 4.1 and figure 4.2, both filled and unfilled ternary skutterudites have lower factor factors, meaning the low electrical conductivity is dominant in power factors. It is also clear in figure 4.1 and figure 4.2that the power factors of ternary skutterudites are comparable with $CoSb_3$ in n-type regions but much lower in the p-type regions. This suggests that their potential for p-type TE materials is much less than for n-type TE materials.

While it may be possible to adjust the carrier concentration of ternary skutterudites to optimize the power factor, it seems very difficult to surpass the values of classical $CoSb_3$. The calculations show the upper limits of transport properties. This study provides valuable information about wide composition screening in ternary skutterudites.

4.1.2 Conclusion

Although the low electrical conductivity significantly limits the power factor of ternary skutterudites, their high Seebeck coefficients and low thermal conductivity [40] are still interesting for further studies. Filled ternary skutterudites could become very useful in thermoelectric applications if we could find some

way to increase their electrical conductivity either through doping or filling voids. We conclude that based on band structure analysis electrical conductivity is limited for a wide range of doping scenarios. So the only parameter that can be optimized is the relaxation time, which we do not compute here. It is likely difficult to increase the relaxation time, given the polar nature of these compositions.

4.2 Stability and Synthesis

All our results shown above are based on theoretical calculations. They are still waiting to be confirmed by experiments. Although some of those ternary skutterudites, such as $CoGe_{1.5}Te_{1.5}$, $CoGe_{1.5}S_{1.5}$, $CoGe_{1.5}Se_{1.5}$, $CoSn_{1.5}Te_{1.5}$ and $CoSn_{1.5}Se_{1.5}$, have already been synthesized and reported, there is no report on synthesis of filled ternary skutterudites to our knowledge [40-45]. High temperature methods are usually applied in the synthesis of skutterudite compounds. Powder mixtures of the elements are heated and cooled down in some container under vacuum using a specific protocol [54]. The structure and composition of the synthesized material can only be measured after the experiment by X-ray diffraction. Thus the synthesis process can be long and hard to predict. Here we present a simple method for qualitatively predicting the stability of a compound using ab initio calculations. This method can provide some theoretical guide towards the difficulty degree of synthesis.

4.2.1 Stability Test

To estimate the stability of a compound, we compare its formation energy with the formation energies of all other compounds that can be formed by the same elements. The formation energy of a compound is the difference between its energy and the total energy of its elements in their simple substance. If the formation energy of our test compound is higher than that of a combination of other compounds with the same number of atoms for each element, it means our test compound is unstable. Because it will release energy when it is turned into other compounds. Otherwise, if the formation energy of our test compound is lower than that of any combination of other compounds with the same number of atoms for each element, it means the test compound is stable.

To conduct such a stability test, we first find all known compounds that are formed by the same elements as our test compound, using the Inorganic Crystal Structure Database [55]. Second, we perform ab initio calculation on each compound with the same set of pseudopotential, k grid, and cutoff energy. Third, we extract their formation energies and create a N-dimension convex hull with those formation energies. N is the number of elements in our test compound. The convex hull for a set of points X, also known as convex envelope, is the minimal convex set containing X in a real vector space V. Figure 4.3 shows a 2-D convex hull for a set of points.

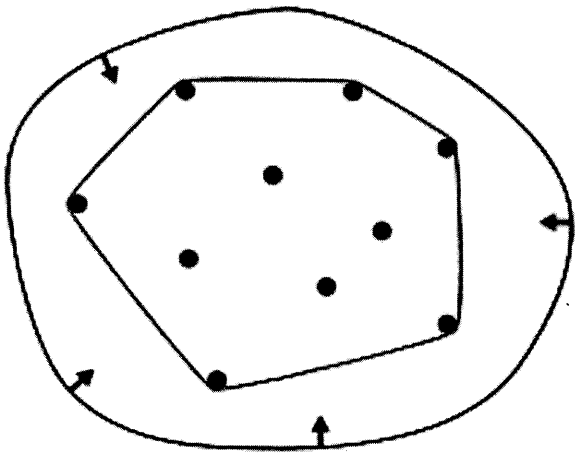

Figure 4.3 An example of convex hull in 2-D. The convex hull is shown in blue in the figure.

The last step is to calculate the formation energy of the test compound and put it in the same vector space as the convex hull. If the test compound is inside the convex hull, it is unstable. If the test compound is outside of the convex hull and is below the convex hull along the energy axis, it is stable. The basic steps of a stability analysis are shown in figure 4.4.

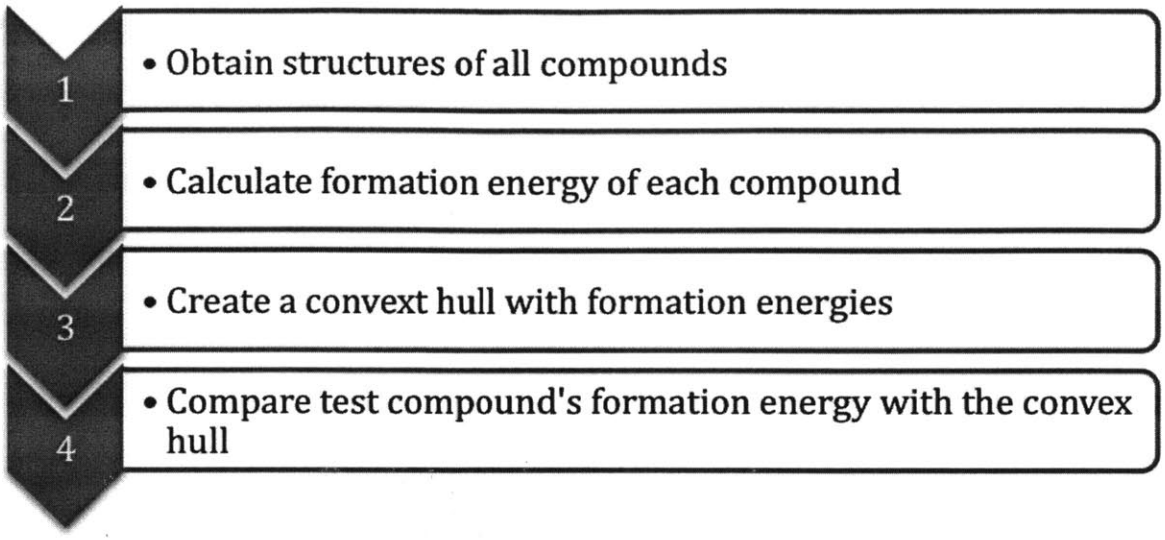

Figure 4.4 Steps for Stability Analysis

4.2.2 Stability Test for $CoGe_{1.5}Te_{1.5}$ and $LaCo_8Ge_{12}Te_{12}$

Our stability analysis requires calculation of the energies of all compounds that are formed by the same elements as the test compound. The number of calculations required increases exponentially with the number of elements in the test compound. Therefore the stability analysis can require large computation time when you have a complex compound to test.

Here we show our calculation process of the stability analysis for $CoGe_{1.5}Te_{1.5}$ and La filled $CoGe_{1.5}Te_{1.5}$. The energy calculation results of all compounds formed by Co, Ge, and Te is listed in table 4.1. The convex hull is shown in figure 4.5. In figure 4.5, the vertical axis is the formation energy. Our calculated formation energy of $CoGe_{1.5}Te_{1.5}$ is below the convex hull, which means it should

be stable. And successful synthesis of $CoGe_{1.5}Te_{1.5}$ in experiment has confirmed this [46].

Table 4.1 Energy calculation results for compounds formed by Co, Ge, and Te. Different structures may correspond to the same compositions.

Chemical Formula	Energy (eV)
Co_4	-296.8913
Ge_8	-64.0559
Te_4	-65.8212
Ge_4Te_4	-97.9125
Ge_3Te_3	-72.9256
Co_2Te_2	-181.3928
Co_2Te_4	-214.0186
Co_8Ge_8	-658.1530
Co_8Ge_{16}	-722.2480
Co_4Ge_2	-312.9696
$Co_{10}Ge_{14}$	-853.8726
$Co_8Ge_8Te_8$	-789.9875
$Co_8Ge_{12}Te_{12}$	-887.9914

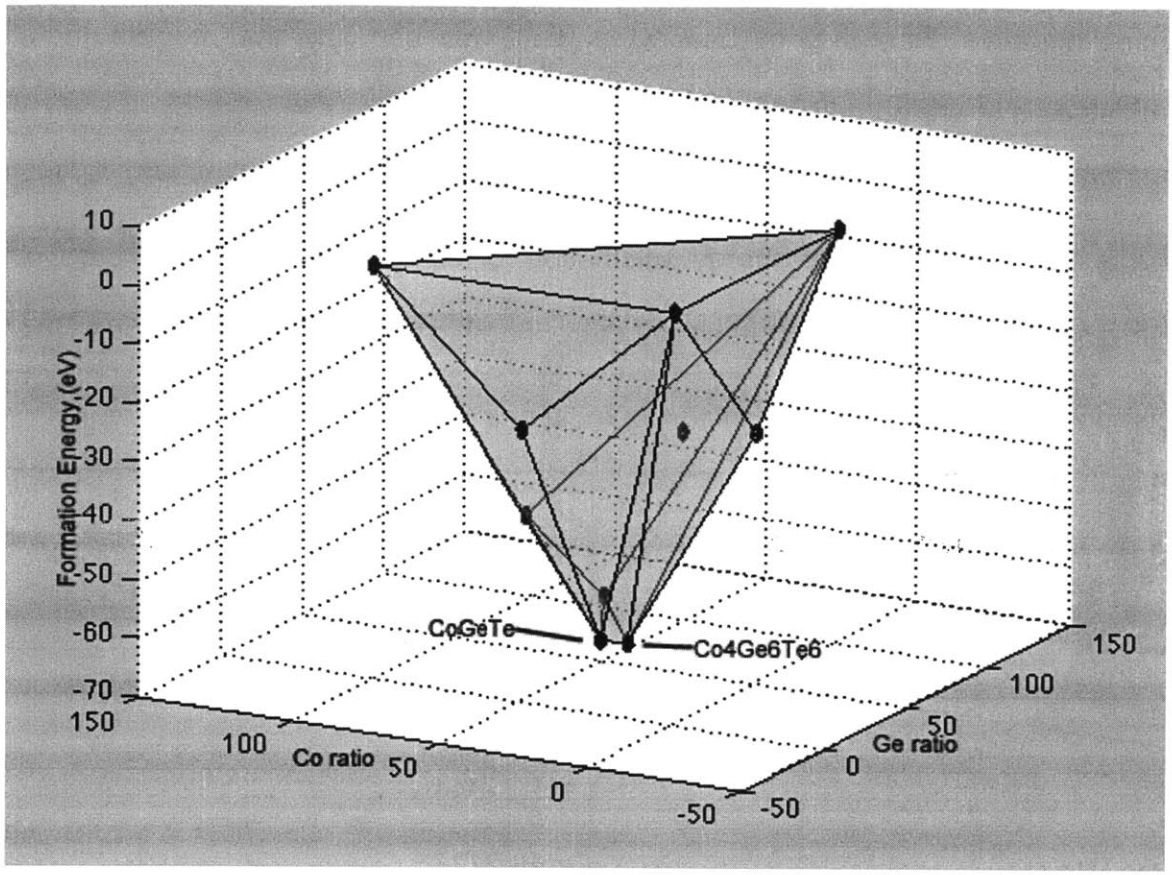

Figure 4.5 Convex hull of formation energies for $CoGe_{1.5}Te_{1.5}$. The vertical axis is the formation energy.

In our analysis on the stability of La filled $CoGe_{1.5}Te_{1.5}$, we calculate the formation energies of all compounds formed by La, Co, Ge, and Te. The results are summarized in table 4.2. Because the convex hull is 4-D, we cannot visualize it in 3-D space. Instead, we plot their formation energies in figure 4.6 and relative stabilities in figure 4.7. The relative stability is defined as the energy difference between a compound and its corresponding point on the closest surface of the convex hull. The negative relative stability of La filled $CoGe_{1.5}Te_{1.5}$ means that it is probably not stable in nature. Since the relative stability of $La_2Co_8Ge_{12}Te_{12}$ is

more negative than that of $La_1Co_8Ge_{12}Te_{12}$, we can say that it gets more unstable as the filling ratio increases.

Table 4.2 Summary of energy calculation for compounds formed by La, Co, Ge, and Te. Different structures may correspond to the same compositions. The compounds of interest are La filled $CoGe_{1.5}Te_{1.5}$.

Chemical Formula	Energy (eV)
La_4	-394.6251
Co_2	-148.8327
Ge_8	-165.59271
Te_4	-65.32644
Ge_4Te_4	-148.2117
Co_2Te_2	-181.50254
Co_2Te_4	-213.9819
Co_8Ge_8	-761.14055
Co_8Ge_{16}	-926.76837
Co_4Ge_2	-339.08377
$Co_{10}Ge_{14}$	-1033.41959
$Co_8Ge_8Te_8$	-891.94305
$Co_8Ge_{12}Te_{12}$	-1040.24925
$La_2Co_2Ge_6$	-470.7750
$La_2Co_4Ge_4$	-578.1811

$La_8Co_4Ge_8$	-1248.18597
$La_{12}Co_4$	-1481.5928
$LaCo_5$	-470.67476
$La_{10}Ge_6$	-1111.5487
La_4Ge_4	-477.9137
La_4Ge_8	-560.8061
$La_{12}Te_{16}$	-1448.5040
La_2Te_4	-263.2686
La_4Te_4	-460.88426
$La_2Co_8Ge_{12}Te_{12}$	-1237.83921
$LaCo_8Ge_{12}Te_{12}$	-1139.06119

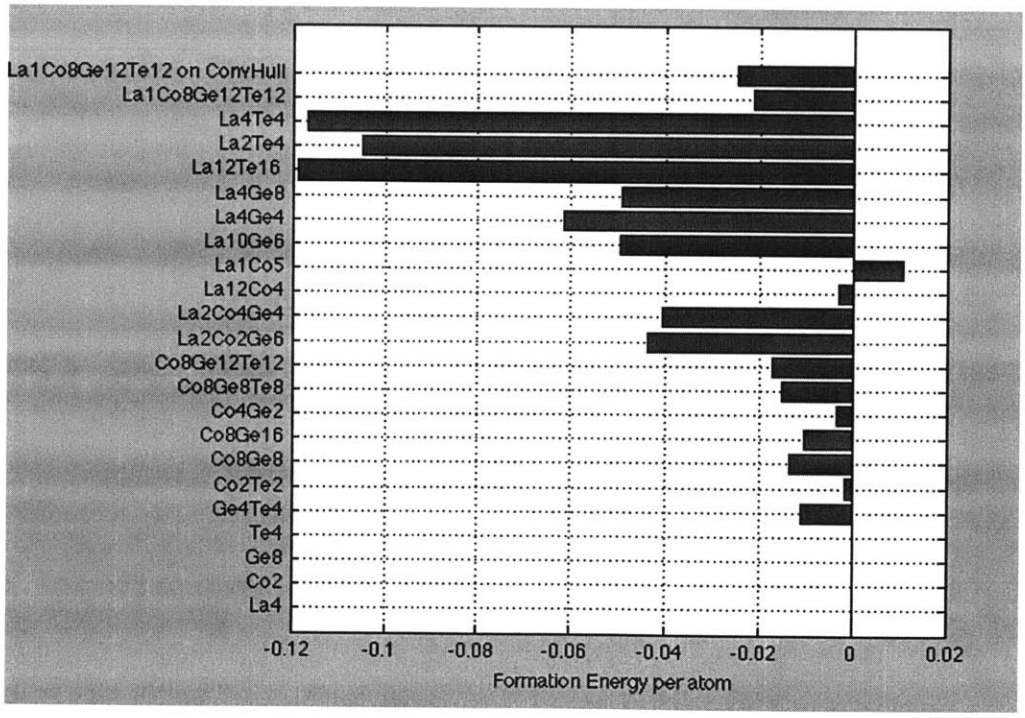

Figure 4.6 Formation energies of all compounds formed by La, Co, Ge, and Te

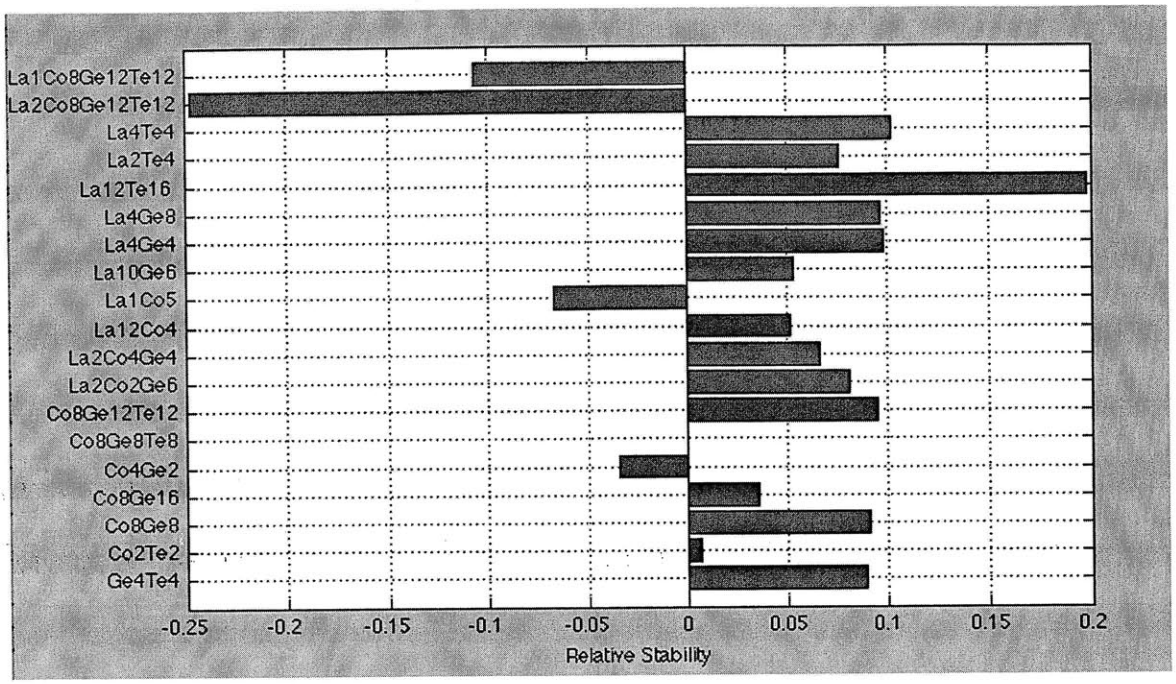

Figure 4.7 Relative stabilities of all compounds formed by La, Co, Ge, and Te. La filled $CoGe_{1.5}Te_{1.5}$ have negative values. Negative values means instability.

Chapter 5: Conclusion and Future Work

5.1 Summary and Conclusion

In this thesis, we investigate the potential of ternary skutterudites as thermoelectric materials through first-principles calculation. Ternary skutterudites share similar crystal and electronic structures with binary skutterudites. Several ternary skutterudites have been synthesized and reported but limited work has been done on the transport properties of filled ternary skutterudites.

We use an ab initio approach to study the electronic and transport properties of both filled and unfilled ternary skutterudites, exploring systematically the composition space of the skutterudites structure. Chapter 2 explains the methodology in this thesis. The optimized structure of each compound is first obtained through relaxation. Then electronic structures are obtained through SCF and NSCF calculations. Transport properties are calculated using BoltzTraP under the assumption of constant relaxation time.

Calculations $CoSn_{1.5}Se_{1.5}$, $CoSn_{1.5}Te_{1.5}$, $CoGe_{1.5}S_{1.5}$, $CoGe_{1.5}Se_{1.5}$, and $CoGe_{1.5}Te_{1.5}$ show relatively high Seebeck coefficients and low electrical conductivities for both unfilled and filled ternary skutterudites in Chapter 3. Ba, Ca, Sr, and La are used as void fillers in our calculation. Unfilled ternary

skutterudites shows higher Seebeck coefficients than $CoSb_3$. Filling with alkaline-earth metals tends to reduce the Seebeck coefficients but they are still higher than $CoSb_3$. Unfilled ternary skutterudites have at most half electrical conductivity as CoSb3 under the assumption of the same constant relaxation time. Filling has no large effect on electrical conductivity for most ternary skutterudites, and in fact decreases it in the p-type region.

Chapter 4 presents the power factors of ternary skutterudites, and we find that they are reduced by low electrical conductivity. Although they have relatively low power factors, we believe ternary skutterudites are still interesting for research as they have low thermal conductivities according to experimental results [48], which may result in good ZT values. We also introduce a method for determine the stability of compounds by calculating formation energies. By applying this method on $CoGe_{1.5}Te_{1.5}$ and La filled $CoGe_{1.5}Te_{1.5}$, the results confirm the stability of $CoGe_{1.5}Te_{1.5}$ in nature and suggest that 50% La filled $CoGe_{1.5}Te_{1.5}$ is not stable.

5.2 Future Work

This thesis provides theoretical data for ternary skutterudites. To complete the computational investigation of this family, future efforts may include other chemical substitutions on the transition metal and filler sites. Using the tools and

infrastructure developed in this thesis, such studies can be performed in an automated fashion. On the experimental side, future work may focus on synthesizing some of the filled ternary skutterudites and measuring their transport properties for comparison. Other filler atoms and filling methods, such as double filling, could also be used for reducing the thermal conductivity.

References:

[1] Interational Energy Agency, *World Energy Outlook 2006 Edition*, 2006

[2] G.Q. Zhang, Q.X. Yu, X.G. Li, Wet chemical synthesis and thermoelectric properties of V-VI one- and two-dimensional nanostructures, *Dalton Transactions*, 39,993-1004,2010

[3] C. Wood, *Materials for thermoelectric energy conversion*, Rep. Prog. Phys. 51.459-539, 1988

[4] Chuang Yu, K.T. Chau, Thermoelectric automotive waste heat energy recovery using maximum power point tracking , *Energy Conversion and Management*, 50.6 , June 2009

[5] Snyder, G. Jeffrey, Application of the compatibility factor to the design of segmented and cascaded thermoelectric generators, *Applied Physics Letters*, v84,2436-2438, Mar 2004

[6] Francis J. DiSalvo, Thermoelectric Cooling and Power Generation, *Science* 285, no. 5428, 703 -706, July 1999

[7] Applications of Thermoelectric Modules. Retrieved July 31, 2011, from http://sctbnord.com/article.php?id=152&rus=0

[8] A.W. Van Herwaarden, P.M. Sarro, Thermal sensors based on the Seebeck effect, *Sensors and Actuators*, 10, 321-346, 1986

[9] Rowe, D.M. *Handbook of Thermoelectrics*, CRC Press, 1995

[10] Terry M. Tritt, Hoeley and Unholey Semiconductors, *Science* ,283.5403, 804-805, Feb 1999

[11] Jones William, March Norman H., *Theoretical Solid State Physics.* Courier Dover Publications, 1985

[12] Tritt, T. M.; Subramanian, M. A., Thermoelectric Materials, Phenomena, and. Applications: A Bird's Eye View. *MRS Bulletin* 2006, 31, (3), 188-194

[13] R.O. Jones, O. Gunnarson, The density functional formalism, its applications and prospects. *Rev.Mod.Phys.* 61(3),689-756, July 1989

[14] P. Hobenberg and W.Kohn. Inhomogeneous Electron Gas. *Phys.Rev.* 136 (3B), B864 B871, November 1964

[15] W. Kohn and L. J. Shan. Self-Consistent Equations Including Exchange and Correlation Effects. *Phys. Rev.* 140(4A),A1133-A1138, November 1965

[16] J. P. Perdew and A. Zunger. Self-interaction Correction to Desnity-functional Approximation for many-electron systems. *Phys. Rev. B* v23.5048, May 1981

[17] W.E.Pickett, Pseudopotential methods in condensed matter applications, *Computer Physics Reports* 9, 115-198,1989

[18] G. B. Bachelet, D. R. Hamann, M. Schlüter, Pseudopotentials that work: From H to Pu, *Phys. Rev. B* v26.8, 4199–4228, October 1982

[19] D. Vanderbilt, Soft self-consistent pseudopotentials in a generalized eigenvalue formalism ,*Phys. Rev. B* v41.11, 7892–7895, April 1990

[20] G. Madsen, D. Singh, *Comput. Phys. Commun.* 2006 175, 67

[21] P. B. Allen, W. W. Schulz, *Phys. Rev. B* 47, 14434–14439, 1993

[22] P. B. Allen, W. E. Pickett, H. Krakauer, *Phys. Rev. B* 37,7482–7490, 1987

[23] D. J. Singh, I. I. Mazin, *Phys. Rev. B* 56, 1650–1653, 1997

[24] T. J. Scheidemantel, C. Ambrosch-Draxl, T. Thonhauser, J. V.Badding, and J. O. Sofo, Transport coefficients from first-principles calculations, *Phys. Rev. B* 68, 125210, 2003

[25] A. F. May, D. J. Singh, and G. J. Snyder, Influence of band structure on the large thermoelectric performance of lanthanum telluride, *Phys. Rev. B* 79153101, 2009 .

[26] L. Bertini and C. Gatti, The impact of the actual geometrical structure of a thermoelectric material on its electronic transport properties: The case of doped skutterudite systems, J. *Chem. Phys.* 121, 8983, 2004

[27] L. Chaput, P. Pecheur, J. Tobola, and H. Scherrer, Transport in doped skutterudites: Ab initio electronic structure calculations, *Phys. Rev. B* 72, 085126, 2005

[28] L. Lykke, B. B. Iversen, and G. K. H. Madsen, Electronic structure and transport in the low-temperature thermoelectric CsBi4Te6: Semiclassical transport equations, *Phys. Rev. B* 73, 195121 2006

[29] J. Yang, H.M. Li, W. Zhang, L.D. Chen, and J.H. Yang, Evaluation of Half-Heusler Compounds as Thermoelectric Materials Based on the Calculated Electrical Transport Properties, *Advanced Functional Materials.* V18,2880-2888, (2008)

[30] P. Giannozzi etc, QUANTUM ESPRESSO: a modular and open-source software project for quantum simulations of materials, *Phys. Condens. Matter* 21.395520, 2009

[31] D. G. Luenberger, *Linear and Nonlinear Programming*, 2nd ed. Kluwer Academic, Norwell, MA, 2003

[32] Oftedal, I. (1928): *Zeitschrift für Kristallographie* 66: 517-546

[33] K. Momma and F. Izumi, *J. Appl. Crystallogr.* 41.653, 2008

[34] Slack G. A.; Tsoukala, V. G. , Some properties of semiconducting $IrSb_3$, *J.Appl. Phys.* 1994, 76, 1665

[35] G. S. Nolas, D. T. Morelli, and T. M. Tritt, Annu. Rev. *Mater.Sci.* 29, 89 1999

[36] Sales, B. C.; Chakoumakos, B. C.; Mandrus, D. *Phys. ReV. B* 2000, 61, 2475

[37] Sales, B. C.; Mandrus, D.; Chakoumakos, B. C.; Keppens, V.;Thompson, J. R. *Phys. ReV. B* , 56.15081, 1997

[38] T. He, J. Chen, H.D. Rosenfeld, M. A. Subramanian, Thermoelectric Properties of Indium-Filled Skutterudites, *Chem. Mater.*,18(3),759-762, 2006

[39] J. Graff, S. Zhu, T. Holgate, J.Y. Peng, J. He, T.M. Tritt, High-Temperature Thermoelectric Properties of Co4Sb12 – Based Skutterudites with Multiple Filler Atoms:Ce0.1InxYbyCo4Sb12, *Electronic Materials*, v40, 696-701,2011

[40] R. Korestein, S. Soled, A. Wold, G. Collin, *Inorg. Chem.* 16.2344, 1977

[41] A. Kjeshus, D.G. Nicholson, T. Rakke, *Acta Chem. Scand.* 27.1315, 1973

[42] A. Lyons, R.P. Gurska, C. Case, S.N. Subbarao, A. Wold, *Mater. Res. Bull.* 13.125, 1978

[43] H.D. Lutz, G. Kliche, J. *Solid State Chem.* 40.64, 1981

[44] J.-P. Fleurial, T. Caillat, A. Borshchevsky, *Proceedings of the 16th International Conference on Thermoelectrics, Dresden*, Germany,1997

[45] M. Partik, C. Kringe, H.D. Lutz, Z. Kristallogr. 211.304, 1996

[46] P.Vaqueiro, G.G.Sobany, A.V.Powell, K.S. Knight, Structure and thermoelectric properties of the ordered skutterudites CoGe1.5Te1.5, *Journal of Solid State Chemistry* 179, 2006

[47] L. Chaput, P. Pecheur, J. Tobola, H. Scherrer, Transport in doped skutterudites: Ab initio electronic structure calculations, *Phys. Rev. B*. 72.085126, 2005

[48] F.Laufek, J.Navratil, J.Plasil, T.Plechacek, C.Drasar, Synthesis, crystal structure and transport properties of skutterudite-related $CoSn_{1.5}Se_{1.5}$, *Journal of Alloys and Compounds* 479, 2009

[49] D. Singh, M. Du, Properties of alkaline-earth-filled skutterudite antimonides, *Phys. Rev. B*, 82, 2010

[50] D.J.Singh, I.I.Mazin, Calculated thermoelectric properties of La-filled skutterudites, *Phys. Rev. B 56*, 4 1997

[51] G.S.Nolas, J.L.Cohn, G.A.Slack, Effect of partial void filling on the lattice thermal conductiveity of skutterudites

[52] D.Wee, B. Kozinsky, N. Marzari, M. Fornari, Effects of filling in CoSb3: Local structure, band gap, and phonons from first principles, *Phys. Rev. B81*, 2010

[53] G.A. Slack, in: D.M. Rowe (Ed.), *CRC Handbook of Thermo- electrics*, Chemical Rubber, Boca Raton, FL, 1995

[54] Ned T. Steston, Susan M. Kauzlarich, Hakon Hope, The synthesis and structure of two filled skutterudite compounds: $BaFe_4Sb_{12}$ and $BaRu_4Sb_{12}$, *Journal of Solid State Chemistry*, v91.1, 140-147, March 1991

[55] Bergerhoff, G. & Brown, I.D. in „Crystallographic Databases", F.H. Allen et al. (Hrsg.) Chester, International Union of Crystallography, (1987).

[56] Sebastian Volz, *Thermal Nanosystems and Nanomaterials*, Springer-Verlag Berlin Heidelberg, 2009

[57] H. J. Goldsmid, A. R. Sheard, and D. A. Wright (1958). "The performance of bismuth telluride thermojunctions". Br. J. Appl. Phys. 9: 365.